NK cell receptor NKG2D sets activation threshold for the NCR1 receptor early in NK cell development

Jelenčić, Vedrana; Šestan, Marko; Kavazović, Inga; Lenartić, Maja; Marinović, Sonja; Holmes, Tim D.; Prchal-Murphy, Michaela; Lisnić, Berislav; Sexl, Veronika; Bryceson, Yenan T.; ...

Source / Izvornik: **Nature Immunology, 2018, 19, 1083 - 1092**

Journal article, Published version
Rad u časopisu, Objavljena verzija rada (izdavačev PDF)

https://doi.org/10.1038/s41590-018-0209-9

Permanent link / Trajna poveznica: https://urn.nsk.hr/urn:nbn:hr:184:508103

nature immunology

ARTICLES

https://doi.org/10.1038/s41590-018-0209-9

NK cell receptor NKG2D sets activation threshold for the NCR1 receptor early in NK cell development

Vedrana Jelenčić[1], Marko Šestan[1,5], Inga Kavazović[1,5], Maja Lenartić[1], Sonja Marinović[1], Tim D. Holmes[2], Michaela Prchal-Murphy[3], Berislav Lisnić[1], Veronika Sexl[3], Yenan T. Bryceson[2,4], Felix M. Wensveen[1] and Bojan Polić[1*]

The activation of natural killer (NK) cells depends on a change in the balance of signals from inhibitory and activating receptors. The activation threshold values of NK cells are thought to be set by engagement of inhibitory receptors during development. Here, we found that the activating receptor NKG2D specifically set the activation threshold for the activating receptor NCR1 through a process that required the adaptor DAP12. As a result, NKGD2-deficient (*Klrk1*$^{-/-}$) mice controlled tumors and cytomegalovirus infection better than wild-type controls through the NCR1-induced production of the cytokine IFN-γ. Expression of NKG2D before the immature NK cell stage increased expression of the adaptor CD3ζ. Reduced expression of CD3ζ in *Klrk1*$^{-/-}$ mice was associated with enhanced signal transduction through NCR1, and CD3ζ deficiency resulted in hyper-responsiveness to stimulation via NCR1. Thus, an activating receptor developmentally set the activity of another activating receptor on NK cells and determined NK cell reactivity to cellular threats.

NK cells detect and eliminate 'stressed' cells, for example, following infection or malignant transformation[1]. Because of their ability to respond without prior sensitization, activation of NK cells needs to be tightly regulated to ensure proper immunosurveillance while avoiding hyperactivity that may lead to inflammatory or autoimmune disorders. Proper responsiveness is mediated through an 'education' process during NK cell development[2]. After engagement of inhibitory receptors, NK cells gain full reactivity and develop tolerance toward self. NK cell responsiveness is further fine-tuned by continuous cues that mature NK cells encounter in the periphery. NK cell activation depends on a shift in the signaling balance between inhibitory and activating receptors. Under homeostatic conditions, inhibitory signals prevail when NK cells interact with peripheral tissues. In response to a cellular threat, host cells downregulate MHCI molecules and/or overexpress stress-induced or nonself-ligands. Upon encounter of 'stressed' target cells, a lack of signals through the inhibitory receptors and/or increased stimulation of activating receptors shifts the balance toward NK cell activation[3]. The factors that control the bandwidth of the equilibrium between inhibitory and activating cues are not completely characterized.

NKG2D and NCR1 are activating receptors expressed on all NK cells. They primarily mediate tissue stress surveillance by recognizing stress-induced self-ligands on target cells[4]. NCR1 (NKp46) is the only member of the NCR family expressed in mice. The role of NCR1 and NKG2D in the control of tumors and infection is well documented[4,5]. Beyond its effector functions[6], NKG2D is expressed from the earliest precursors onward during NK cell development[7,8]. NKG2D-deficient mice have bone marrow (BM) NK cell progenitors that have enhanced proliferation, faster maturation and augmented sensitivity to apoptosis[9], indicating a role for NKG2D signaling in NK cell development. Moreover, as expected, NKG2D deficiency results in reduced NK cell responsiveness to target cells expressing NKG2D ligands[9,10]. However, in response to specific activating stimuli, NKG2D-deficient NK cells display a hyper-reactive phenotype in terms of production of the cytokine IFN-γ[9,11] and better control mouse cytomegalovirus (mCMV) infection compared to NKG2D-sufficient NK cells[9]. How NKG2D deficiency drives NK cell hyper-reactivity is unclear.

The activating receptors NCR1 and NKG2D require adaptors to convert signals into the cell. NKG2D associates with the adaptors DAP10 or DAP12 (ref. [12]), and NCR1 docks the adaptors CD3ζ and FcεRγ[13]. DAP10 has a YxxM motif through which the PI3K and Grb2-Vav1-SOS1 are engaged[13]. CD3ζ, FcεRγ and DAP12 possess ITAM motifs, whose phosphorylation activates signaling proteins Syk and ZAP70, resulting in cytotoxicity and/or cytokine production[13]. It is commonly believed that adaptors with ITAM motifs only transduce activating signals. However, increasing evidence shows that they can also negatively impact signaling cascades[13–15]. How adaptors of activating NK cell receptors contribute to negative regulation of signaling is mostly unknown.

Here we demonstrate that NKG2D deficiency or blocking of NKG2D signaling early during NK cell development caused hyper-reactivity of the NCR1 receptor, resulting in enhanced control of mCMV infection and tumors expressing NCR1 ligands. Deficiency of NKG2D or DAP12 resulted in downregulation of CD3ζ and ZAP-70 yet stronger signaling after NCR1 stimulation. Ablation of NKG2D in immature CD122^{+}NK1.1^{+}NCR1^{+}CD11b^{-}c-Kit^{-} NK cells completely abrogated the hyperactive phenotype of NK cells, indicating that this regulation occurs early during NK development.

[1]Department of Histology and Embryology, Faculty of Medicine, University of Rijeka, Rijeka, Croatia. [2]Center for Hematology and Regenerative Medicine, Department of Medicine Huddinge, Karolinska Institutet, Stockholm, Sweden. [3]Institute of Pharmacology and Toxicology, Department for Biomedical Sciences, University of Veterinary Medicine Vienna, Vienna, Austria. [4]Broegelmann Laboratory, Department of Clinical Sciences, University of Bergen, Bergen, Norway. [5]These authors contributed equally to this work: Marko Šestan, Inga Kavazović. *e-mail: bojan.polic@medri.uniri.hr

NKG2D-driven regulation of NCR1 signaling was independent of conventional education mechanisms. Altogether, these results reveal an unknown developmental regulation of one activating NK receptor by another, which controls the sensitivity of immune surveillance of tumors and viral infections.

Results

***Klrk1*$^{-/-}$ NK cells efficiently control tumors negative for NKG2D ligands.** We addressed whether *Klrk1*$^{-/-}$ mice, which are NKG2D deficient, can control tumors that do not express NKG2D ligands using a radiation-induced thymic lymphoma (RITL) model[16]. In this model, mice receive low-dose irradiation early in life and develop disease after 3 months. RITL is characterized by expansion of CD4$^+$CD8$^+$ T cells lacking NKG2D ligands (Supplementary Fig. 1a,b). When *Klrk1*$^{-/-}$ and C57BL/6J mice were exposed to this regime, we observed a delay in the onset of disease in *Klrk1*$^{-/-}$ mice. Notably, whereas penetration of RITL was around 80% 7 months after irradiation in C57BL/6J mice, less than half of all *Klrk1*$^{-/-}$ mice developed disease (Fig. 1a). To substantiate this observation, C57BL/6J and *Klrk1*$^{-/-}$ mice were injected i.v. with B16-F10 (B16) melanoma cells, which induce lung metastases after i.v. injection or solid tumors when applied subcutaneously[17] and do not express NKG2D ligands (Supplementary Fig. 1b). We observed a delay in the development of disease in *Klrk1*$^{-/-}$ mice compared to *Klrk1*$^{+/+}$ littermates (Fig. 1b and Supplementary Fig. 1c). B16 cells applied subcutaneously showed a reduced rate of tumor growth in *Klrk1*$^{-/-}$ mice relative to *Klrk1*$^{+/+}$ littermates (Fig. 1c and Supplementary Fig. 1d), indicating better control of cancer-cell expansion in *Klrk1*$^{-/-}$ mice.

Because NKG2D is expressed on subsets of T cells[6], we asked whether NKG2D deficiency enhanced T cell-mediated control of tumors in *Klrk1*$^{-/-}$ mice. *Klrk1*$^{fl/fl}$ mice[18] were crossed with *Cd4*^{Cre} mice to ablate NKG2D on CD4$^+$ T cells, CD8$^+$ T cells and NKT cells (Supplementary Fig. 1e). No differences were observed in the survival of *Cd4*^{Cre}*Klrk1*$^{fl/fl}$ mice and *Klrk1*$^{fl/fl}$ littermates in the RITL model (Supplementary Fig. 1f). In addition, i.v. injection of B16 cells did not result in survival differences between *Cd4*^{Cre}*Klrk1*$^{fl/fl}$ mice and *Klrk1*$^{fl/fl}$ littermates (Fig. 1d). However, *Klrk1*$^{-/-}$ mice in which NK cells were depleted by monoclonal antibodies (mAb) 1 d before i.v. injection of B16 cells no longer had a survival advantage over C57BL/6J control mice (Fig. 1e). Also, differences in tumor growth between Klrk1$^{-/-}$ mice and C57BL/6J controls after s.c. injection of B16 cells were lost following NK cell depletion (Fig. 1f). NK cells can also limit tumor growth indirectly by controlling T cell priming and expansion[19,20]. *Klrk1*$^{-/-}$ mice in which depletion of CD4$^+$ or CD8$^+$ T cells by mAb started 1 d before i.v. injection of B16 cells had prolonged survival in comparison to C57BL/6J mice (Fig. 1g and Supplementary Fig. 1g), indicating that NK cells are mediating the survival effect of *Klrk1*$^{-/-}$ mice independently of T cells. Splenic *Klrk1*$^{-/-}$ NK cells killed B16 target cells with efficiency equal to that of C57BL/6J NK cells in 4 h (Fig. 1h) and 14 h (Supplementary Fig. 1h) in vitro cytotoxicity assays. PMA + ionomycin-stimulated splenic NK cells predominantly produced IFN-γ (Fig. 1i), a cytokine that promotes tumor surveillance[21]. *Klrk1*$^{-/-}$ NK cells produced more IFN-γ than *Klrk1*$^{+/+}$ NK cells after 24 h in co-culture with B16 cells (Fig. 1j). To corroborate this finding in vivo, *Ifng* mRNA was quantified in tumors isolated from C57BL/6J or *Klrk1*$^{-/-}$ mice 10 d after s.c. injection of B16 cells. Tumors isolated from *Klrk1*$^{-/-}$ mice had higher expression of *Ifng* mRNA than those from C57BL/6J mice (Supplementary Fig. 1i). To confirm the role of IFN-γ in tumor control, we crossed *Ifng*$^{-/-}$ mice with *Klrk1*$^{-/-}$ mice and followed the survival of *Ifng*$^{-/-}$, *Klrk1*$^{-/-}$ and *Klrk1*$^{-/-}$*Ifng*$^{-/-}$ mice following i.v. injection of B16 melanoma cells. *Klrk1*$^{-/-}$*Ifng*$^{-/-}$ mice did not have a survival advantage compared to *Ifng*$^{-/-}$ mice, whereas *Klrk1*$^{-/-}$ mice did (Fig. 1k), indicating that better control of B16 melanoma was mediated by an increased capacity of *Klrk1*$^{-/-}$ NK cells to produce IFN-γ.

***Klrk1*$^{-/-}$ NK cells have specific hyper-reactivity through NCR1.** To analyze the impact of NKG2D deficiency on target-cell engagement, we performed a conjugation assay with B16 melanoma[22]. We observed no difference in the amount of NK target cell complexes between C57BL/6J and *Klrk1*$^{-/-}$ NK cells (Fig. 2a). To test whether increased IFN-γ production in *Klrk1*$^{-/-}$ NK cells resulted from enhanced signaling through activating receptors, we stimulated splenic NK cells from *Klrk1*$^{-/-}$ mice or *Klrk1*$^{+/+}$ littermates through different activating receptors. Engagement of receptors NK1.1, DNAM-1, Ly49D or Ly49H by mAb or incubation of NK cells with IL-12 and IL-18 cytokines resulted in similar production of IFN-γ in *Klrk1*$^{-/-}$ and *Klrk1*$^{+/+}$ NK cells (Fig. 2b,c and Supplementary Fig. 1j). In contrast, stimulation with mAb against the NCR1 receptor resulted in a higher percentage of IFN-γ$^+$*Klrk1*$^{-/-}$ NK cells compared to IFNγ$^+$*Klrk1*$^{+/+}$ NK cells (Fig. 2b,c). NCR1 expression and stimulation-induced degranulation by mAb (Fig. 2d) were similar in *Klrk1*$^{-/-}$ and *Klrk1*$^{+/+}$ NK cells. Thus, NKG2D-deficient NK cells show hyper-responsiveness to stimulation through the NCR1 receptor.

NCR1 is known to have a role in the control of B16 melanoma[23,24]. Labeling with NCR1-Ig fusion proteins[25] showed high expression of NCR1 ligands on B16 cells (Supplementary Fig. 1k). To investigate whether NCR1 was involved in the enhanced tumor control by *Klrk1*$^{-/-}$ mice, we used *Ncr1*$^{GFP/GFP}$ mice, which are deficient in NCR1. *Ncr1*$^{GFP/GFP}$ mice showed reduced survival in comparison to C57BL/6J mice after i.v. injection of B16 melanoma cells (Fig. 2e). *Klrk1*$^{-/-}$ mice showed better survival in comparison to C57BL/6J controls, whereas *Klrk1*$^{-/-}$*Ncr1*$^{GFP/GFP}$ mice had survival comparable to that of *Ncr1*$^{GFP/GFP}$ mice (Fig. 2e). Depletion of NK cells by mAb abrogated any difference in survival between all mice (Fig. 2e). These results show that the enhanced tumor control in *Klrk1*$^{-/-}$ mice is dependent on NCR1 engagement by NK cells.

Compared to C57BL/6J mice, *Klrk1*$^{-/-}$ mice have better control of MCMV infection (Supplementary Fig. 2), which is NK cell dependent[9]. To test whether this effect was mediated through NCR1, we infected C57BL/6J, *Ncr1*$^{GFP/GFP}$, *Klrk1*$^{-/-}$ and *Ncr1*$^{GFP/GFP}$*Klrk1*$^{-/-}$ mice with Δ*m157* MCMV, a mutant strain of MCMV lacking ligand for NK cell receptor Ly49H. We used this MCMV strain to avoid the Ly49H-mediated control of viral replication, which may occlude the effects of NCR1 (ref. [26]). *Klrk1*$^{-/-}$ mice showed better control of Δ*m157* MCMV in the spleen compared to all other mice, and this was lost after depletion of NK cells by mAb (Fig. 2f). These results show that the enhanced control of MCMV infection by NKG2D-deficient mice is dependent on NCR1 engagement by NK cells.

NKG2D sets NCR1 activation threshold during NK cell development. During NK cell development, NKG2D is expressed from the Lin$^-$CD117^{dim}Sca1^{2+}Flt3L$^-$CD127$^+$ cells onwards, which represents the earliest NK cell committed precursor (pre-pro NK)[7]. Because NKG2D deficiency impacts development of NK cells in the bone marrow (BM)[9] as well as NK cells effector responses in the periphery[27,28], we asked whether the hyper-reactivity of *Klrk1*$^{-/-}$ NK cells to NCR1 stimulation was acquired during development or later on in mature NK cells in the periphery. We crossed *Klrk1*$^{fl/fl}$ mice with *Ncr1*^{Cre} mice (Supplementary Fig. 3a) to generate *Ncr1*^{Cre}*Klrk1*$^{fl/fl}$ mice, in which Cre-mediated deletion of *Klrk1* occurs in CD122$^+$NK1.1$^+$NCR1$^+$CD11b$^-$c-Kit$^-$ NK cells[7,29]. Spleen NK cells from *Ncr1*^{Cre}*Klrk1*$^{fl/fl}$ mice showed comparable production of IFN-γ to *Klrk1*$^{fl/fl}$ littermates after stimulation of NCR1 by mAb in vitro (Fig. 3a). We did not observe differences in survival between *Ncr1*^{Cre}*Klrk1*$^{fl/fl}$ mice and *Klrk1*$^{fl/fl}$ littermates after i.v. injection of B16 cells (Fig. 3b). In contrast, a higher percentage of spleen NK cells from *Klrk1*$^{Δ/Δ}$ mice, which had a germline deletion of *Klrk1* and were generated from the cross between deleter (tg-*cmv*^{Cre})[30] and *Klrk1*$^{fl/fl}$ mice, produced IFN-γ to NCR1 stimulation by mAb

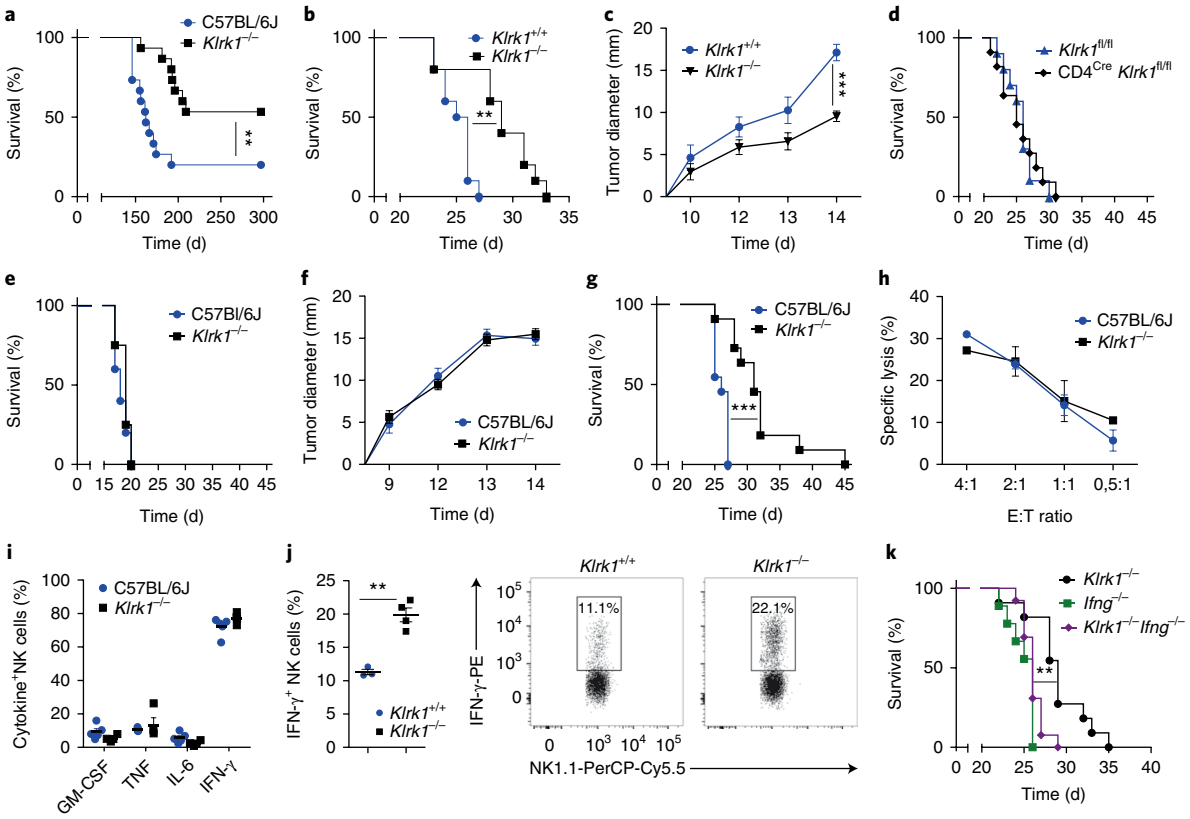

Fig. 1 | Better control of B16 melanoma by *Klrk1*$^{-/-}$ mice is NK cell and IFNγ mediated. (**a**) Survival curve of C57BL/6 J and *Klrk1*$^{-/-}$ mice in a model of radiation-induced thymic lymphomas. (**b**–**g**) Graphs show survival curves (**b**,**e**,**g**) or tumor sizes (**c**,**f**) of *Klrk1*$^{-/-}$ mice and indicated controls after injection of B16 cells i.v (**b**,**e**,**g**) or s.c. (**c**,**f**). One day prior to tumor inoculation, mice were either untreated (**b**,**c**) or received depleting antibodies directed against NK cells (**e**,**f**) or CD8$^+$ T cells (**g**). Depletion was repeated every fifth day. (**d**) Survival curve of *Klrk1*$^{fl/fl}$ and CD4^{Cre}*Klrk1*$^{fl/fl}$ mice that received B16 cells i.v. (**h**) Killing capacity of NK cells from C57BL/6 J or *Klrk1*$^{-/-}$ mice toward CFSE-labeled B16 cells after 4 h of co-cultivation at indicated effector to target (E:T) ratios. (**i**), Cytokine production by NK cells from C57BL/6 J or *Klrk1*$^{-/-}$ mice 4 h after stimulation with PMA/ionomycin. (**j**) IFN-γ production by NK cells after co-cultivation of splenocytes from *Klrk1*$^{+/+}$ and *Klrk1*$^{-/-}$ mice with B16 cells. Boxed areas are gated for IFN-γ$^+$ cells. (**k**) Survival curve of *Ifng*$^{-/-}$, *Klrk1*$^{-/-}$*Ifng*$^{-/-}$ and *Klrk1*$^{-/-}$ mice after B16 cells i.v. injection. Graphs for tumor experiments (**a**–**g**,**k**; $n = 10$ mice per group) are representative of two independent experiments. Survival curves were analyzed by the Kaplan–Meier model followed by log-rank (Mantel–Cox) test (two-tailed; $^{**}P < 0.01$, $^{***}P < 0.001$). Tumor sizes and difference between groups after stimulations were analyzed using two-tailed unpaired *t*-test (shown mean ± s.e.m.); $^{**}P < 0.01$. Results in (**h**,**i**,**j**) ($n = 5$ mice per group) are representative of two independent experiments. (**b**–**d**,**j**) were performed using littermates.

compared to C57BL/6 J control (Supplementary Fig. 3b). These results indicate that NKG2D sets the activation threshold for NCR1 developmentaly before CD122+NK1.1+NCR1+CD11b− c-Kit− NK cells.

Next we tested whether NKG2D played a role during early NK cell development in a model independent of genetic modification of *Klrk1*. In *Rag1*^{Cre}*EYFP*$^{Stop\text{-}Flox}$iDTR mice, all cells derived from Rag1$^+$ hematopoietic precursors, including T cells, B cells and a large fraction of NK cells, expressed EYFP and dipheteria toxin receptor (DTR) upon Cre-mediated deletion of the transcriptional 'stop' sequence and can be eliminated by diphtheria toxin (DT) injection (Supplementary Fig. 3c). *Rag1*^{Cre}*EYFP*$^{Stop\text{-}Flox}$iDTR mice were i.p. injected with DT on the first two consecutive days to deplete all NK cells originating from the Rag1$^+$ precursors. To inhibit NKG2D signaling on all newly generated NK progenitors, the mice were treated from the second day onward with NKG2D-blocking mAb or isotype control (Supplementary Fig. 3c), and the receptor responsiveness of EYFP$^+$ NK cells was analyzed 2 weeks later. Spleen NK cells from *Rag1*^{Cre}*EYFP*$^{Stop\text{-}Flox}$iDTR mice that had received i.v. NKG2D-blocking mAb showed increased IFN-γ production after stimulation of NCR1 but not following stimulation of NK1.1 or Ly49H by mAbs (Fig. 3c), indicating that NKG2D sets the activation threshold for NCR1 early in NK cell development.

These observations prompted us to analyze the impact of NKG2D deficiency on hematopoiesis. NKG2D deficiency does not affect hematopoietic stem cells or more differentiated precursors such as the common lymphoid and myeloid precursors[18,31] (Fig. 3d). However, there was a reduction in the number of BM Lin$^-$CD117^{dim}Sca1^{2+}Flt3L$^-$CD127$^+$ NK progenitors in *Klrk1*$^{-/-}$ mice compared to *Klrk1*$^{+/+}$ littermates (Fig. 3d). Further analysis of NK cell development revealed an increase in percentage of CD122$^+$NK1.1$^+$NCR1$^-$CD11b$^-$c-Kit$^-$ and decrease of CD122$^+$NK1.1$^+$NCR1$^+$CD11b$^-$c-Kit$^-$ NK progenitors in *Klrk1*$^{-/-}$ mice compared to *Klrk1*$^{+/+}$ littermates (Fig. 3e and Supplementary Fig. 4a). To confirm the role of NKG2D in changing NK progenitors in a second model, we analyzed them in BM of *Rag1*^{Cre}*EYFP*$^{Stop\text{-}Flox}$iDTR mice 15 d after DT injection and treatment with NKG2D-blocking mAb. Similar to *Klrk1*$^{-/-}$ mice, we observed an increase in percentage of CD122$^+$NK1.1$^+$NCR1$^-$CD11b$^-$c-Kit$^-$ and decrease of CD122$^+$NK1.1$^+$NCR1$^+$CD11b$^-$c-Kit$^-$ NK progenitors compared to isotype control-treated *Rag1*^{Cre}*EYFP*$^{Stop\text{-}Flox}$iDTR mice (Fig. 3f). Together, these results indicate a role of NKG2D in NK cell development at the time of NCR1 appearance on NK progenitors.

NKG2D-mediated NK cell-education differs from known mechanisms. NK cells that never expressed Rag1 during

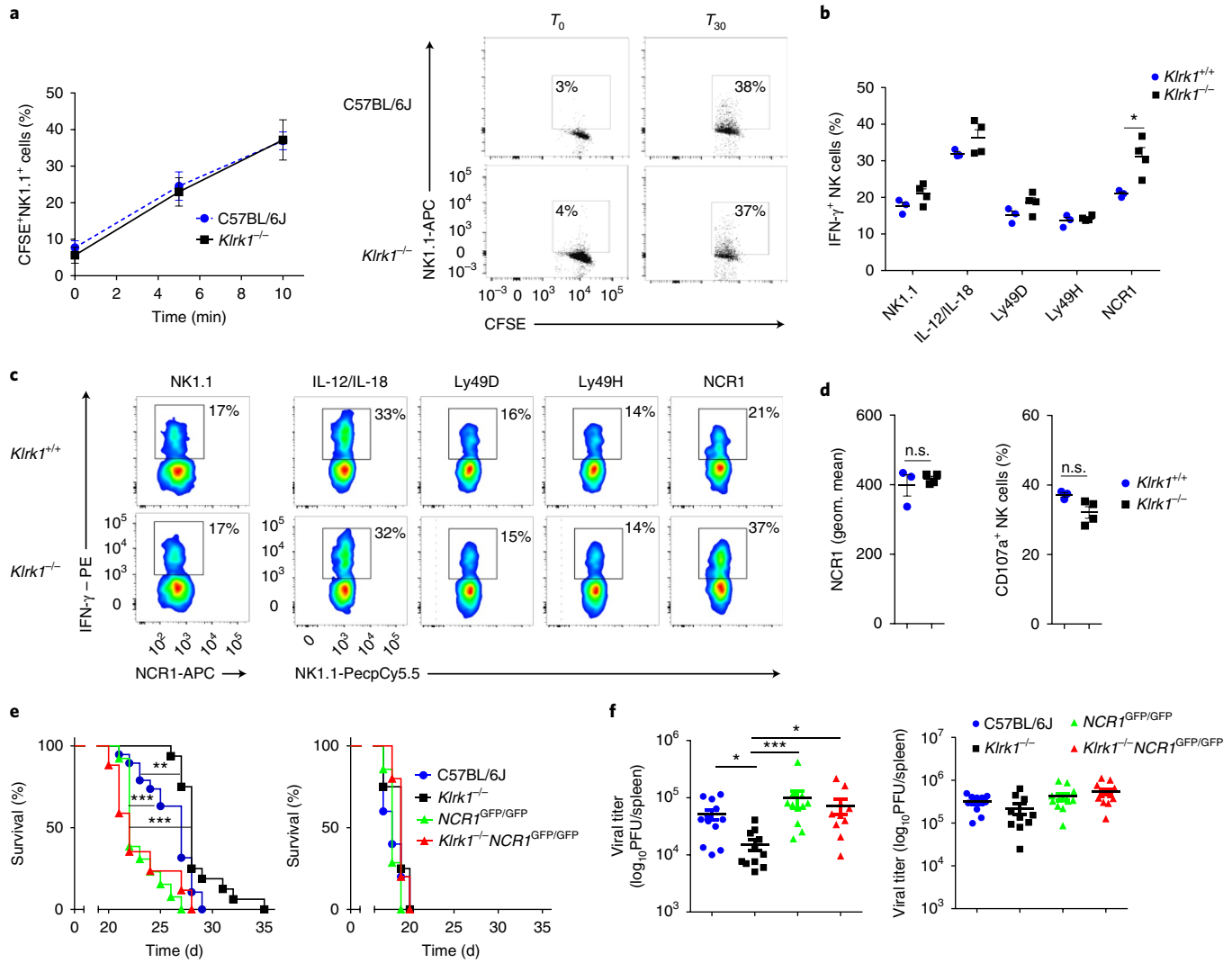

Fig. 2 | *Klrk1*$^{-/-}$ NK cells show specific hyper-reactivity through NCR1 receptor. (**a**) Representative graph (left) and dot plots (right) from three independent experiments showing formation of conjugates between labeled NK and B16 cells (mean ± s.e.m.; $n = 5$ mice per group). (**b**) IFN-γ production by NK cells from *Klrk1*$^{+/+}$ ($n = 3$) or *Klrk1*$^{-/-}$ ($n = 4$) mice after stimulation by monoclonal antibodies (mAb) through the indicated receptors or with IL-12/IL-18 cytokines. (**c**) Representative FACS plots gated for CD3$^-$NCR1$^+$ cells (NK1.1 stimulation) or CD3$^-$NK1.1$^+$ cells (other stimuli). (**d**) Levels of NCR1 expression from untreated cells (left) and percentage of CD107a$^+$ (right) NK cells after 4 h of NCR1 stimulation using mAb, from *Klrk1*$^{+/+}$ ($n = 3$) or *Klrk1*$^{-/-}$ ($n = 4$) mice. (**e**) Survival curves for untreated (left) or NK cell depleted (right) indicated groups of mice after B16 i.v. injections ($n = 10$ mice per group). Representative graph from three independent experiments. (**f**) Viral titers in spleens 4 d after infection of indicated group of mice with 5×10^5 PFU *Δm157* MCMV. Mice were left untreated (left) or received NK cell depleting antibodies one day before infection (right). Graphs show pooled data from two independent experiments. Survival curves were analyzed by the Kaplan–Meier model followed by log-rank (Mantel–Cox) test (two-tailed; $^{**}P < 0.01$, $^{***}P < 0.001$). **a**,**b** and **d** are analyzed using two-tailed unpaired *t*-test (shown mean ± s.e.m.; n.s., not significant, $^{*}P < 0.05$). Viral titers were analyzed using Kruskal–Wallis test (shown mean ± s.e.m.; $^{*}P < 0.05$; $^{***}P < 0.001$). **b**–**d** show representative data from two independent experiments using littermates.

development showed cell-intrinsic hyper-responsiveness in comparison to NK cells generated from Rag1$^+$ progenitors[32]. We therefore asked whether NKG2D promoted NK cell development from a Rag1$^+$ progenitor. We generated *Klrk1*$^{+/+}$*Rag1*^{Cre}*EYFP*$^{Stop\text{-}Flox}$ and *Klrk1*$^{-/-}$ *Rag1*^{Cre}*EYFP*$^{Stop\text{-}Flox}$ mice, in which expression of Rag1 was marked through the expression of EYFP. As shown previously[32], we observed that a higher percentage of EYFP$^-$ NK cells from *Klrk1*$^{+/+}$*Rag1*^{Cre}*EYFP*$^{Stop\text{-}Flox}$ mice were Klrg1$^+$ and CD11b$^+$ compared to EYFP$^+$ NK cells (Supplementary Fig. 4b). We made the same observations in *Klrk1*$^{-/-}$ *Rag1*^{Cre}*EYFP*$^{Stop\text{-}Flox}$ mice (Supplementary Fig. 4c). However, there were no differences in percentages of EYFP$^+$ or EYFP$^-$ NK cells between *Klrk1*$^{+/+}$*Rag1*^{Cre}*EYFP*$^{Stop\text{-}Flox}$ and *Klrk1*$^{-/-}$ *Rag1*^{Cre}*EYFP*$^{Stop\text{-}Flox}$ mice (Fig. 3g). Furthermore, regardless of EYFP expression, NK cells from *Klrk1*$^{-/-}$*Rag1*^{Cre}*EYFP*$^{Stop\text{-}Flox}$ mice produced more IFN-γ than NK cells from *Klrk1*$^{+/+}$*Rag1*^{Cre}*EYFP*$^{Stop\text{-}Flox}$ mice upon NCR1 stimulation by mAb, whereas responsiveness to NK1.1 was similar (Fig. 3h), indicating that NKG2D influences NCR1 signaling independently of the Rag-driven developmental pathway.

To investigate the role of Ly49-mediated education in NCR1 signaling, we compared the production of IFN-γ in Ly49I$^+$ to that in Ly49I$^-$ *Klrk1*$^{+/+}$ and *Klrk1*$^{-/-}$ NK cells following NCR1 stimulation by mAb. *Klrk1*$^{-/-}$ Ly49I$^+$ NK cells produced more IFN-γ in comparison to *Klrk1*$^{+/+}$ Ly49I$^-$ NK cells (Fig. 3i). However, *Klrk1*$^{-/-}$ NK cells produced more IFN-γ compared to *Klrk1*$^{+/+}$ NK cells regardless of their Ly49I expression (Fig. 3i). Also, there was no difference in the frequency of Ly49I$^+$ NK cells between *Klrk1*$^{-/-}$ and *Klrk1*$^{+/+}$ cells (Supplementary Fig. 4d). These observations indicate that the

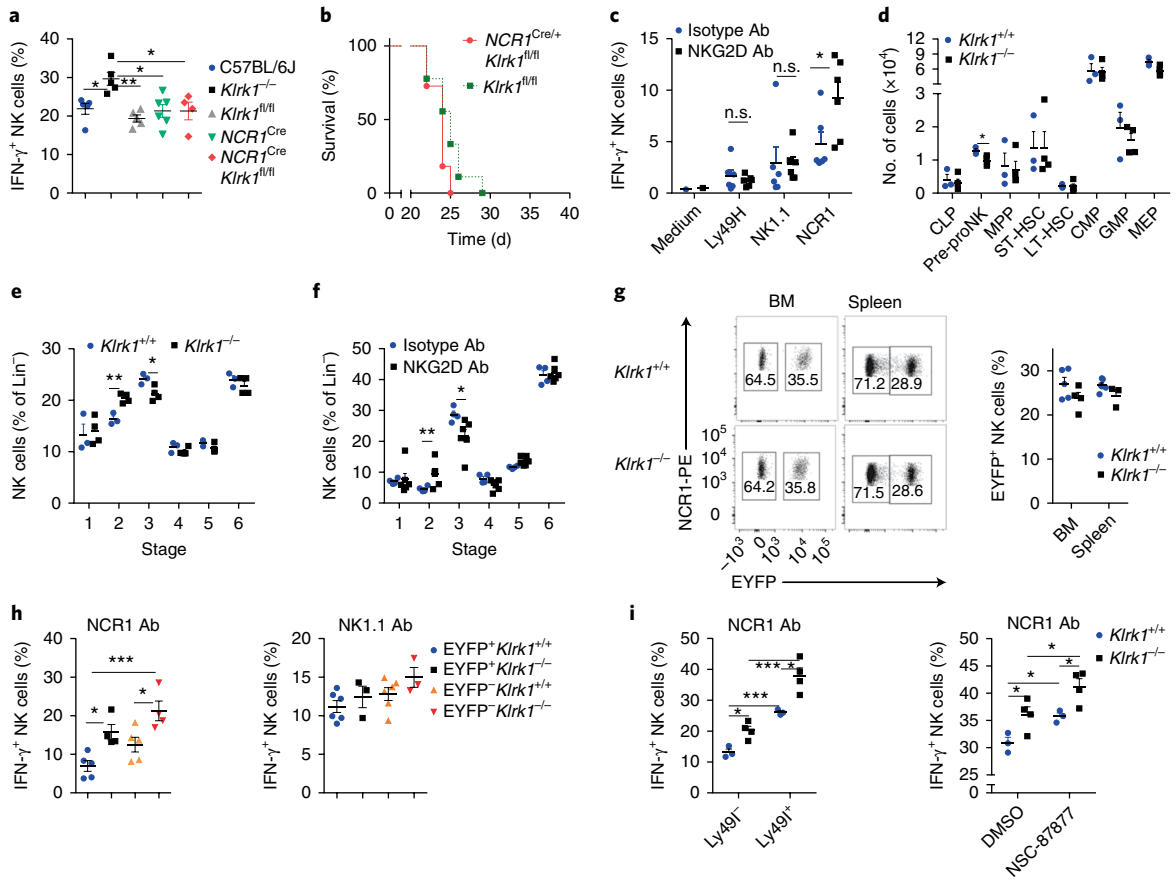

Fig. 3 | NKG2D sets an activation threshold for NCR1 early during NK cell development in a process that differs from known mechanisms of NK cell education. (**a**) IFNγ production by NK cells from C57BL/6 J, *Klrk1*$^{-/-}$, *Klrk1*$^{fl/fl}$ ($n=5$ mice per group), *NCR1*^{Cre} ($n=6$), and *NCR1*^{Cre} *Klrk1*$^{fl/fl}$ ($n=4$) mice after 4 h of NCR1 stimulation using mAb (ANOVA, with Bonferroni's post-test correction). (**b**) Survival curve for *Ncr1*^{Cre}*Klrk1*$^{fl/fl}$ and *Klrk1*$^{fl/fl}$ littermates after B16 i.v. injection (Kaplan–Meier model followed by log-rank (Mantel–Cox) test; $n=10$ mice per group). c,f, Analysis of splenic EYFP$^+$ NK cells from Rag^{Cre}*EYFP*$^{Stop\text{-}Flox}$iDTR mice injected with DT and NKG2D-blocking antibodies or isotype controls ($n=6$ mice per group). (**c**) IFN-γ production after 4 h of indicated stimulations. (**f**) Developmental NK cell stages in the BM (see Supplementary Fig. 4a). (**d**,**e**) Hematopoietic precursor populations (**d**) and development of NK cells (**e**) were analyzed in BM of *Klrk1*$^{-/-}$ ($n=4$) and *Klrk1*$^{+/+}$ ($n=3$) littermates. g,h, Analysis of EYFP expression (**g**) and IFN-γ production by NK cells after indicated stimulations in *Rag1*^{Cre}*EYFP*$^{Stop\text{-}Flox}$*Klrk1*$^{+/+}$ ($n=5$ for NCR1 or 6 for NK1.1 stimulation) and *Rag1*^{Cre}*EYFP*$^{Stop\text{-}Flox}$ *Klrk1*$^{-/-}$ ($n=3$ for NK1.1 or 4 for NCR1 stimulation) (**h**). Gates indicate EYFP$^+$ and EYFP$^-$ populations. (**i**), NK cells from *Klrk1*$^{-/-}$ ($n=4$) and *Klrk1*$^{+/+}$ ($n=3$) littermates were stimulated through the NCR1 receptor using mAb and IFN-γ production was analyzed after 4 h. Cells were untreated and gated based on Ly49I expression (left) or stimulation was performed in presence of SHP1/2 inhibitor (NSC-87877) or solvent only (right). c–g were analyzed using two-tailed unpaired *t*-test and h–i using ANOVA, with Bonferroni's post-test correction. Shown are means ± s.e.m. of representative plots (*$P<0.05$, ** $P<0.01$, *** $P<0.001$) of two (**b**,**c**,**d**,**e**,**f**,**i**) or four (**a**,**g**,**h**) experiments.

threshold for the NKG2D-dependent activation of NCR1 is independent of Ly49-mediated education.

SHP-1 plays a role in NK cell education, and SHP-1-deficient NK cells are hypo-responsive to MHCI-deficient transplants and tumors[33,34]. To test whether SHP-1 played a role in the NKG2D-mediated education, we treated *Klrk1*$^{-/-}$ and *Klrk1*$^{+/+}$ spleen NK cells in vitro with the SHP-1/2 inhibitor NSC-87877 (ref. [35]) and then stimulated them through the NCR1 receptor by mAb. SHP-1/2 inhibition resulted in an increase of IFN-γ production in both *Klrk1*$^{-/-}$ and *Klrk1*$^{+/+}$ NK cells. However, production of IFN-γ was higher in *Klrk1*$^{-/-}$ NK cells compared to *Klrk1*$^{+/+}$ (Fig. 3i), indicating that NKG2D sets the activation threshold for NCR1 independently of SHP-1/2.

The NKG2D-DAP12 signaling axis regulates NCR1 activity. To investigate the mechanism through which NKG2D regulates the activity of NCR1, we focused on the adaptors DAP10 and DAP12 (ref. [12]). We used mice lacking either DAP10 (*Hcst*$^{-/-}$) or DAP12 (*Tyrobp*$^{-/-}$). There were no differences in the production of IFN-γ between C57BL/6J, *Klrk1*$^{-/-}$, *Hcst*$^{-/-}$ and *Tyrobp*$^{-/-}$ spleen NK cells after stimulation through NK1.1 by mAb (Fig. 4a). Ly49H and Ly49D use DAP12 for signal transduction[13]. IFN-γ production from *Tyrobp*$^{-/-}$, but not *Klrk1*$^{-/-}$ or *Hcst*$^{-/-}$ NK cells was reduced compared to C57BL/6J NK cells after stimulation through these receptors (Fig. 4a). Notably, after stimulation through NCR1, *Tyrobp*$^{-/-}$, but not *Hcst*$^{-/-}$, NK cells showed an increase in IFN-γ production compared to C57BL/6J controls, similarly to *Klrk1*$^{-/-}$ NK cells (Fig. 4a). Similar observations were made after NCR1 stimulation of spleen NK cells from *Tyrobp*$^{-/-}$ mice and *Tyrobp*$^{+/+}$ littermates (Supplementary Fig. 5a). When B16 cells were injected i.v. in *Klrk1*$^{-/-}$, *Hcst*$^{-/-}$, *Tyrobp*$^{-/-}$ and C57BL/6J mice, *Tyrobp*$^{-/-}$ mice showed prolonged survival in comparison to *Hcst*$^{-/-}$, C57BL/6J and even *Klrk1*$^{-/-}$ mice (Fig. 4b), indicating that signaling through DAP12 only was important for NK cell hyper-reactivity to NCR1 stimulation.

We next questioned whether the hyper-responsiveness of DAP12-deficient NK cells was specific for NKG2D or whether

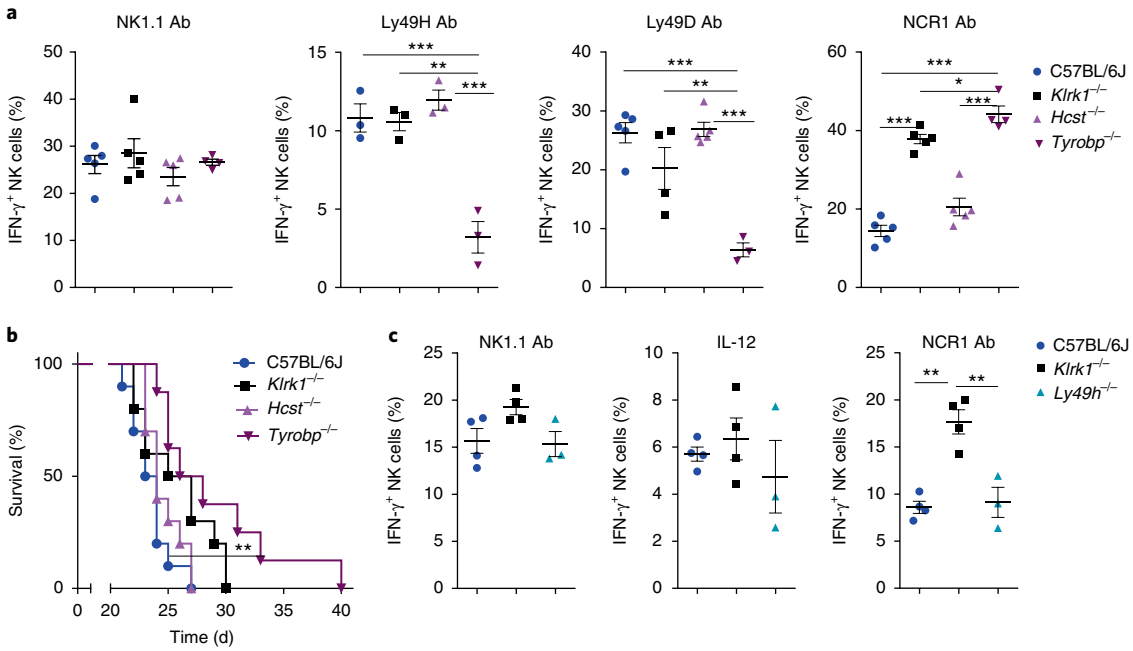

Fig. 4 | The NKG2D-DAP12 signaling axis regulates NCR1 activity. (**a**) NK cells from *Tyrobp*$^{-/-}$ ($n=3$ or 4 mice), *Hcst*$^{-/-}$ ($n=3$ or 5 mice), *Klrk1*$^{-/-}$ ($n=3$ or 5 mice) and C57BL/6 J ($n=3$ or 5) mice were stimulated for 4 h through the NK1.1, Ly49H, Ly49D or NCR1 receptor by mAb and IFN-γ production was analyzed after 4 h. (**b**) Survival curves of indicated groups of mice after i.v. injection of B16 cells (Kaplan–Meier model followed by Log-rank (Mantel-Cox) test; $n=10$ mice per group). (**c**) NK cells from *Ly49h*$^{-/-}$ ($n=3$ mice), *Klrk1*$^{-/-}$ ($n=4$ mice) and C57BL/6J ($n=4$ mice) mice were stimulated through the NK1.1 or NCR1 receptor by mAb or with IL-12 cytokines and IFN-γ production was analyzed after 4 h. Shown are representative plots of three (**a**) or two (**b**,**c**) experiments. For analysis of **a** and **c** ANOVA, with Bonferroni's post-test correction for multiple comparisons was used. Shown are means ± s.e.m. * $P<0.05$, ** $P<0.01$, *** $P<0.001$.

it was observed following deletion of any receptor that signals through this adaptor. When *Klrk1*$^{-/-}$, *Ly49H*$^{-/-}$ or C57BL/6J spleen NK cells were stimulated through NK1.1 or NCR1 by mAbs or with the cytokine IL-12, *Ly49H*$^{-/-}$ NK cells did not show increased IFN-γ production after any of these stimulations relative to C57BL/6J NK cells (Fig. 4c). In mice, NKG2D has a long (L) and a short (S) isoform, of which only the latter associates with DAP12 (ref. [12]). We therefore investigated whether NKG2D-S and DAP12 were expressed during early NK cell development in wild-type mice. qPCR in sorted CD122^{+}NK1.1^{-}NCR1^{-}CD11b^{-}c-Kit^{-} and CD122^{+}NK1.1^{+}NCR1^{-}CD11b^{-}c-Kit^{-} BM NK progenitors detected transcripts for the *Tyrobp* and short isoform of *Klrk1*, whose expression increased from CD122^{+}NK1.1^{-}NCR1^{-}CD11b^{-}c-Kit^{-} to CD122^{+}NK1.1^{+}NCR1^{-}CD11b^{-}c-Kit^{-} NK progenitors (Supplementary Fig. 5b,c). Thus, the NKG2D-mediated control of NCR1 signaling occurs through the NKG2D–DAP12 axis early in NK cell development.

CD3ζ and ZAP-70 are involved in inhibition of NCR1 signaling. Because NCR1 uses CD3ζ and FcεRγ for signal transduction[36], we tested whether the NKG2D-DAP12 axis affects signaling through these adaptors. Flow cytometry analysis indicated that expression of CD3ζ was reduced in both *Klrk1*$^{-/-}$ and *Tyrobp*$^{-/-}$ NK cells in comparison to C57BL/6J NK cells, whereas expression of FcεRγ was comparable in all groups (Fig. 5a,b and Supplementary Fig. 5d,e). In addition, expression of ZAP-70, a signaling component downstream of CD3ζ, was reduced in *Klrk1*$^{-/-}$ and *Tyrobp*$^{-/-}$ spleen NK cells relative to C57BL/6J NK cells, whereas expression of the Syk kinase, also downstream of CD3ζ, was comparable in all groups (Fig. 5a,b and Supplementary Fig. 5e). Immunoblot analysis also showed reduced expression of CD3ζ and ZAP-70 in *Klrk1*$^{-/-}$ spleen NK cells compared to C57BL/6J NK cells (Fig. 5c). In contrast, *Ncr1*^{Cre}*Klrk1*$^{fl/fl}$ spleen NK cells had no alterations in the expression of CD3ζ or ZAP-70 compared to *Klrk1*$^{fl/fl}$ NK cells (Fig. 5d). Because CD3ζ-deficient mouse spleen NK cells are hyper-responsive to CD16 stimulation[15], we asked whether NKG2D and DAP12 mediated the responsiveness of NK cells to CD16 engagement. *Klrk1*$^{-/-}$ and *Tyrobp*$^{-/-}$ spleen NK cells showed enhanced IFN-γ production following CD16 stimulation compared to C57BL/6J NK cells (Supplementary Fig. 5f).

As determined by qPCR, *Cd247* or *Fcre1g* mRNA was similar in *Klrk1*$^{-/-}$ and C57BL/6J NK cells (Fig. 5e), suggesting altered post-transcriptional regulation. To identify candidates that might impact the expression of CD3ζ and/or ZAP-70, we compared the transcriptome of spleen CD3^{-}NK1.1^{+}NCR1^{+} NK cells from C57BL/6J, *Klrk1* $^{-/-}$ and *Tyrobp*$^{-/-}$ mice by RNA sequencing. Ninety-four genes were differentially expressed between C57BL/6J and *Klrk1*$^{-/-}$ NK cells, whereas expression of 543 genes was different between *Tyrobp*$^{-/-}$ and C57BL/6J NK cells (Fig. 6a). We performed qualified cluster analysis of genes differentially expressed in *Klrk1*$^{-/-}$ NK cells versus C57BL/6J cells on the basis of data mining of known protein–protein interactions to establish a potential link with CD3ζ and/or ZAP-70 (Supplementary Fig. 6a). Next, we determined which of these genes showed a shared expression pattern between *Klrk1*$^{-/-}$ and *Tyrobp*$^{-/-}$ mice (Fig. 6a,b). *Prf*, encoding perforin, and *Sla*, encoding adaptor SLAP-1, were identified as potential candidates. Using flow cytometry analysis we did not detect a difference in perforin protein expression between *Klrk1*$^{-/-}$ and C57BL/6J spleen NK cells (Fig. 6c). SLAP-1 is known to target CD3ζ for degradation in thymocytes[37]. *Sla* transcripts were upregulated in *Klrk1*$^{-/-}$ and *Tyrobp*$^{-/-}$ NK cells compared to C57BL/6J NK cells (Fig. 6b). Cell surface expression of SLAP-1 on *Klrk1*$^{-/-}$ NK cells was increased compared to C67BL/6J NK cells (Fig. 6c and Supplementary Fig. 6b). In addition, expression of SLAP-1 in splenic EYFP^{+} NK cells

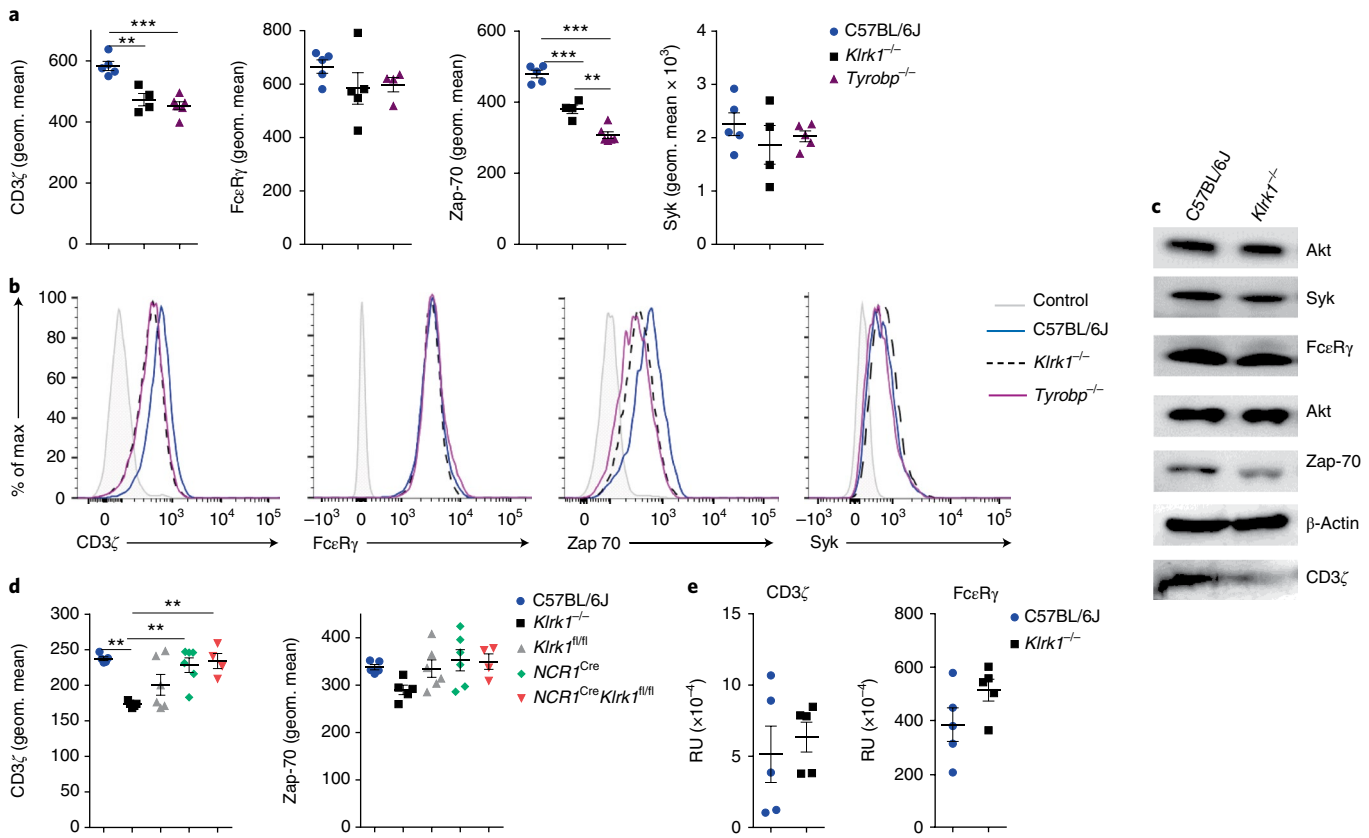

Fig. 5 | *Klrk1*$^{-/-}$ and *Tyrobp*$^{-/-}$ NK cells have reduced levels of CD3ζ and Zap-70 signaling molecules. (**a**,**b**) Splenic NK cells from C57BL/6 J ($n=5$ mice per group), *Klrk1*$^{-/-}$ ($n=4$–5 mice per group) and *Tyrobp*$^{-/-}$($n=4$ or 6 mice per group) mice were analyzed for expression of CD3ζ, FcεRγ, Zap-70 and Syk. Shown are graphs of geometric mean values for indicated molecules (**a**) as well as histograms (**b**). As a controls for staining, isotype control (for CD3ζ and Zap-70), FMO (for FcεRγ) or secondary antibody only (for Syk) were used. FACS plots were gated for NK cells (CD3$^-$NK1.1$^+$). (**c**) NK cells from C57BL/6 J and *Klrk1*$^{-/-}$ mice were sorted and expression of indicated proteins was analyzed by western blot. Pan-akt or β-actin were used as controls for equal loading. (**d**) NK cells from *Ncr1*^{Cre} ($n=6$), *Ncr1*^{Cre}*Klrk1*$^{fl/fl}$ ($n=4$), *Klrk1*$^{-/-}$($n=5$) and C57BL/6 J ($n=5$) mice were analyzed for CD3ζ and Zap-70 expression. Figures show graphs of geometric mean. (**e**) Transcript levels for CD3ζ and FcεRγ of NK cells sorted from spleens from C57BL/6 J and *Klrk1*$^{-/-}$ mice were analyzed by qPCR ($n=5$ mice per group). Shown are representative plots of three (**a**,**c**) or two (**b**,**d**) experiments. ANOVA, with Bonferroni's post-test correction for multiple comparisons was used to analyze **a** and **c**. Two-tailed unpaired *t*-test was used to analyze **d**. Shown are means ± s.e.m. ** $P<0.01$, *** $P<0.001$.

from *Rag1*^{Cre}*EYFP*$^{Stop\text{-}Flox}$iDTR mice 15 d after DT injection and treatment with NKG2D-blocking Ab was increased compared to EYFP$^+$ NK cells from DT and isotype-treated *Rag1*^{Cre}*EYFP*$^{Stop\text{-}Flox}$iDTR mice (Fig. 6d). Next, we asked whether SLAP-1 downregulates CD3ζ in NK cells. We observed increased expression of CD3ζ protein in spleen NK cells from *Sla*$^{-/-}$ mice[37] compared to wild-type controls, whereas expression of NCR1, FcεRγ, Syk and ZAP-70 were not affected (Fig. 6e and Supplementary Fig. 6c). Thus, NKG2D deficiency results in an increase of SLAP-1 protein in NK cells, which reduces the expression of CD3ζ.

In thymocytes, CD3ζ and ZAP-70 mediate activation upon TCR stimulation, but they are also important for the shutdown of signal transduction through recruitment of proteins involved in proximal negative feedback mechanisms[15,38]. We therefore asked whether NCR1 stimulation in *Klrk1*$^{-/-}$ cells results in enhanced proximal signaling. Phosphorylation of Syk, the kinase directly downstream of FcεRγ, was both increased and prolonged in *Klrk1*$^{-/-}$ NK cells after NCR1 stimulation by mAbs compared to *Klrk1*$^{+/+}$ NK cells (Fig. 6f). Similar observations were made in *Tyrobp*$^{-/-}$ cells (Fig. 6g and Supplementary Fig. 6d). Importantly, phosphorylation of PLC-γ, which is a target of Syk, was prolonged in *Klrk1*$^{-/-}$ NK cells compared to *Klrk1*$^{+/+}$ NK cells, whereas maximal phosphorylation of PLC-γ was only slightly increased (Fig. 6h), indicating a reduced negative feedback loop in proximal NCR1 signaling. Finally, we asked whether CD3ζ deficiency resulted in hyper-responsive NK cells. *Cd247*$^{-/-}$ spleen NK cells produced more IFN-γ after stimulation through the NCR1 receptor by mAb, but not through NK1.1, Ly49H or Ly49D, compared to C57BL/6 J spleen NK cells (Fig. 6i), indicating a role for CD3ζ in the negative regulation of NCR1 signaling. NCR1 expression was similar in all the cells analyzed (Supplementary Fig. 6f). As such, NKG2D sets an activation threshold for the NCR1 receptor by increasing CD3ζ protein and by lowering expression of SLAP-1 during NK cell development.

Discussion

Here we show that NKG2D sets activation threshold for NCR1 early in NK cell development, which determines the sensitivity of NK cells to cellular targets expressing NCR1 ligands. This process operates through a NKG2D–DAP12 signaling axis that drives downregulation of CD3ζ and ZAP-70, involved in negative regulation of NCR1 signaling. Thus, we identified a developmental NK cell regulation, distinct from previously described mechanisms of education in which one activating receptor regulates the activity of another activating receptor.

Our results indicated that the role of NKG2D in the regulation of NCR1 activation was mediated by DAP12. Although we did not

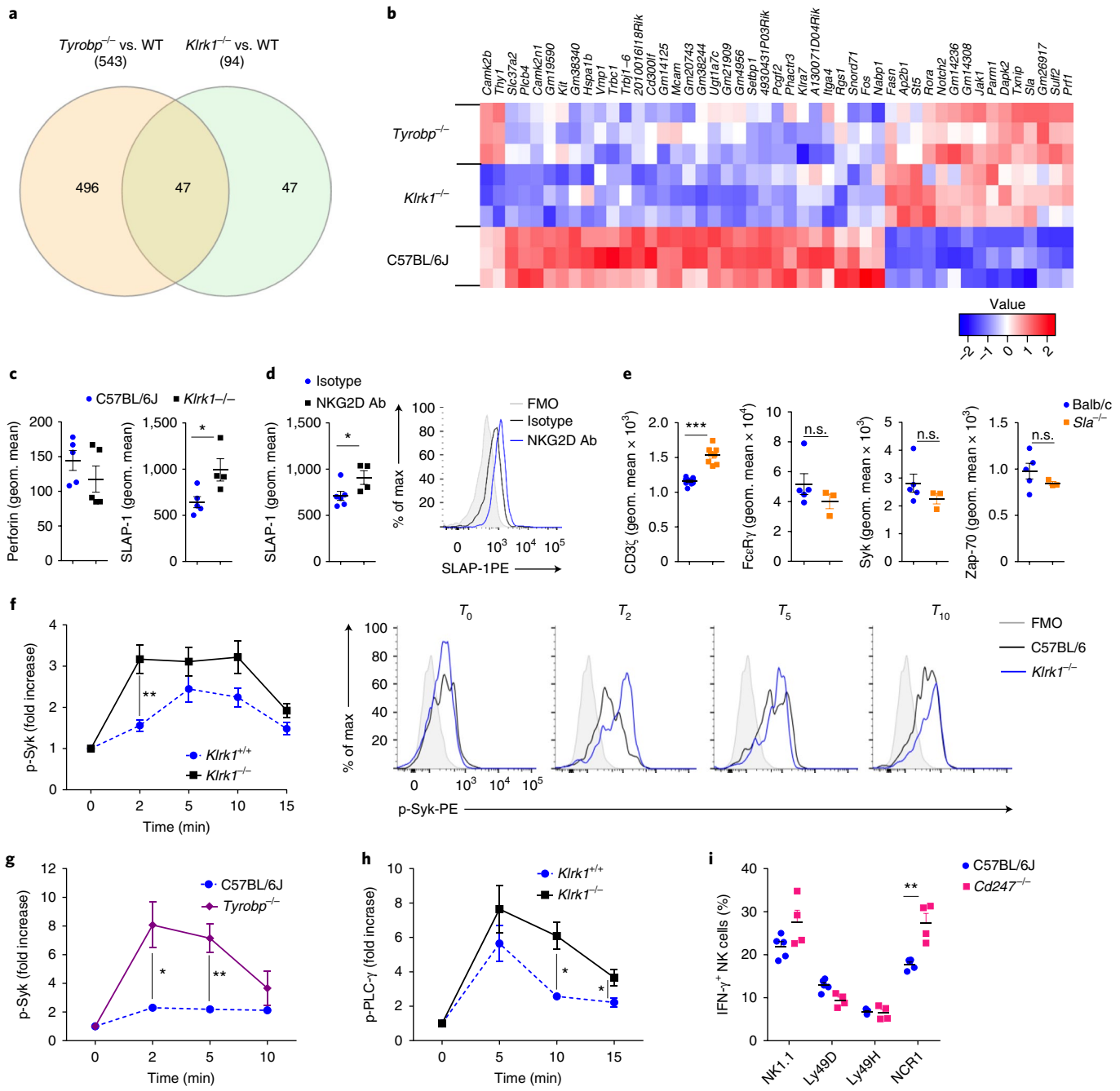

Fig. 6 | Hyper-reactivity of *Klrk1*$^{-/-}$ NK cells in response to NCR1 stimulation is a consequence of reduced expression of CD3ζ. (**a**,**b**) RNAseq was performed on sorted NK cells isolated from the spleens of *Klrk1*$^{-/-}$, *Tyrobp*$^{-/-}$ and C57BL/6 J mice. Venn diagram (**a**) and heat map (**b**) for differentially expressed genes. (**c**) Analysis of splenic NK cells from C57BL/6 J ($n=5$ mice) and *Klrk1*$^{-/-}$ ($n=4$ mice) mice for expression of perforin (left) and SLAP-1 (right). Shown are geometric mean values. (**d**) Analysis of NK cells from Rag^{Cre}*EYFP*$^{Stop\text{-}Flox}$iDTR mice injected with DT and in addition with NKG2D-blocking antibodies ($n=4$ mice) or isotype controls ($n=6$ mice) splenic EYFP^{+} NK cells were analyzed for expression of SLAP-1. FACS plot is gated for NK cells (CD3^{-}NK1.1^{+}). (**e**) Splenic NK cells from Balb/c ($n=5$ mice) and *Sla*$^{-/-}$ ($n=3$ mice) mice were analyzed for expression of Syk, FcεRγ, ZAP-70 and CD3ζ ($n=10$ Balb/c and 8 *Sla*$^{-/-}$ mice). Graphs show geometric mean values. (**f**–**h**) NK cells from C57BL/6 J ($n=4$), *Tyrobp*$^{-/-}$ ($n=4$) *or Klrk1*$^{-/-}$ ($n=5$) mice were stimulated through the NCR1 receptor by mAb and phosphorylation of Syk (**f**,**g**) and PLC-γ (**h**) was analyzed. FACS plots are gated for NK cells (CD3^{-}NK1.1^{+}). (**i**) NK cells from C57BL/6 J and *Cd247*$^{-/-}$ ($n=4$ mice per group) mice were stimulated through NCR1 by mAb and IFN-γ production was analyzed. Shown are representative plots of one (**a**,**b**), two (**d**,**e**,**i**,**h**) or three (**c**,**f**,**g**) experiments. **f** and **h** are performed using littermates. Two-tailed unpaired *t*-test was used to analyze data in **c**–**i**. Shown are means ± s.e.m. * $P<0.05$, ** $P<0.01$, *** $P<0.001$.

formally show that NKG2D and DAP12 were directly engaged to mediate their regulatory role during NK cell development, the absence of a hyper-responsive phenotype in Ly49H-deficient mice makes it highly unlikely that these two molecules have an identical yet independent effect. The role of DAP12 in setting activating thresholds does not appear to be unique to NK cells. DAP12-deficient mice have macrophages[39] and pDCs[40] that produce higher amounts of cytokines after TLR stimulation in comparison to

wild-type mice. The mechanism by which DAP12 sets activation thresholds in these cells is unknown, but it may be similar to the NKG2D-mediated regulation in NK cells. Because human NKG2D does not bind to DAP12, our findings can not be directly extrapolated. However, several KIRs signal through DAP12 (refs [41–44]). It has been shown that activating KIRs downmodulate human NK cell-responsiveness in individuals carrying self ligands[43]. It will therefore be interesting to see whether regulation of NKp46 activation thresholds in humans is regulated through NKG2D or through Dap12-binding KIRs.

Our data indicated the involvement of CD3ζ and ZAP-70 in the negative regulation of NCR1 signaling. NK cells from CD3ζ-deficient mice had higher production of IFN-γ after stimulation through the NCR1 receptor. These observations are in line with reports of an important role for CD3ζ and ZAP-70 in the negative regulation of signaling in T cells[38,45] and NK cells[15]. Following T cell receptor engagement, CD3ζ-ZAP-70 recruit ubiquitinase Nrdp3 and phosphatases Sts-1 and Sts-2, which dephosphorylate ZAP-70 and cause cessation of the activating signal. Deficiency for Nrdp3, Sts-1 and Sts-2 causes prolonged signal transduction[46]. We observed that *Klrk1*$^{-/-}$ mice had delayed signal inhibition following NCR1 stimulation, especially at the level of PLC-γ phosphorylation. Thus, we propose that a reduction in expression of CD3ζ-ZAP-70 causes impaired recruitment of factors that terminate the activating signal directly downstream of the NCR1 receptor. Although a direct interaction between CD16 and CD3ζ has only been shown in human cells, deficiency of CD3ζ or DAP12 causes hyper-reactivity in murine NK cells in response to CD16 stimulation[15,47]. We saw increased production of IFN-γ in *Klrk1*$^{-/-}$ NK cells after stimulation through the CD16 receptor, suggesting that NKG2D may also regulate the responsiveness of CD16.

Chronic exposure to NKG2D ligands can result in cross-tolerance of multiple distinct NK cell activation pathways[27,28]. In addition, weak signaling through NKG2D leads to reduced activity of NK cells, which can be circumvented by administration of soluble high-affinity ligands[28]. However, peripheral 'desensitization' through NKG2D generates a general hyporesponsiveness of NK cells to activating stimuli. Therefore, the developmental and peripheral regulation of activation thresholds by NKG2D appear to use distinct molecular mechanisms.

The NKG2D-mediated 'education' of NCR1 is distinct from previously described mechanisms. Education through molecules such as Ly49 receptors[2] or via modification of the SHP phosphatases[33] results in a general hyporesponsiveness to activating stimuli. The impact of NKG2D-mediated education, in contrast, appears restricted to NCR1. Importantly, we identify a temporal window in which NKG2D permanently controls NCR1 responsiveness. Deletion of *Klrk1* from the CD122^{+}NK1.1^{+}NCR1^{+}CD11b^{-}c-Kit^{-} NK progenitors onward did not cause NK cell hyperresponsivenes to NCR1 as was the case in mice with germline deletion of *Klrk1*. Ly49 molecules are expressed from the CD122^{+}NK1.1^{+}NCR1^{+}CD11b^{-}c-Kit^{-} NK progenitors onward. Indeed, lack of Ly49H, which also signals through DAP12, did not result in NK cell hyperresponsiveness to NCR1. How permanent regulation of CD3ζ expression by NKG2D signaling at a highly restricted stage of NK cell development is accomplished mechanistically remains unclear. Our data suggest that post-transcriptional regulation of CD3ζ. RNA-seq analysis revealed *Sla* as a candidate involved in this process. *Sla* encodes SLAP-1, an adaptor that targets CD3ζ for ubiquitin ligase c-Cbl-dependent degradation following receptor activation[37]. NKG2D deficiency, or blocking of NKG2D during NK cell development, caused a permanent increase in *Sla* gene expression, implying increased degradation of CD3ζ and subsequently altered signal transduction through NCR1. Indeed, SLAP-1-deficient NK cells expressed higher amounts of CD3ζ. CD244, another NK activating receptor expressed on multipotent hematopoietic progenitors[48], was shown to regulate immune cell function through epigenetic silencing of chromatin regions[49]. Although methylation analysis of the *Sla* locus in *Klrk1*$^{-/-}$ NK cells did not reveal differences compared to wild-type NK cells (unpublished data by T.D.H. and Y.C.B.), this does not exclude another ways of epigenetic regulation of *Sla* expression.

Online content

Any methods, additional references, Nature Research reporting summaries, source data, statements of data availability and associated accession codes are available at https://doi.org/10.1038/s41590-018-0209-9.

Received: 3 November 2017; Accepted: 17 August 2018;
Published online: 17 September 2018

References

1. Spits, H., Bernink, J. H. & Lanier, L. NK cells and type 1 innate lymphoid cells: partners in host defense. *Nat. Immunol.* **17**, 758–764 (2016).
2. Elliott, J. M. & Yokoyama, W. M. Unifying concepts of MHC-dependent natural killer cell education. *Trends Immunol.* **32**, 364–372 (2011).
3. Long, E. O., Kim, H. S., Liu, D., Peterson, M. E. & Rajagopalan, S. Controlling natural killer cell responses: integration of signals for activation and inhibition. *Annu. Rev. Immunol.* **31**, 227–258 (2013).
4. Koch, J., Steinle, A., Watzl, C. & Mandelboim, O. Activating natural cytotoxicity receptors of natural killer cells in cancer and infection. *Trends Immunol.* **34**, 182–191 (2013).
5. Zafirova, B., Wensveen, F. M., Gulin, M. & Polić, B. Regulation of immune cell function and differentiation by the NKG2D receptor. *Cell. Mol. Life Sci.* **68**, 3519–3529 (2011).
6. Jelenčić, V., Lenartić, M., Wensveen, F. M. & Polić, B. NKG2D: A versatile player in the immune system. *Immunol. Lett.* **189**, 48–53 (2017).
7. Goh, W. & Huntington, N. D. Regulation of murine natural killer cell development. *Front. Immunol.* **8**, 130 (2017).
8. Huntington, N. D., Vosshenrich, C. A. & Di Santo, J. P. Developmental pathways that generate natural-killer-cell diversity in mice and humans. *Nat. Rev. Immunol.* **7**, 703–714 (2007).
9. Zafirova, B. et al. Altered NK cell development and enhanced NK cell-mediated resistance to mouse cytomegalovirus in NKG2D-deficient mice. *Immunity* **31**, 270–282 (2009).
10. Guerra, N. et al. NKG2D-deficient mice are defective in tumor surveillance in models of spontaneous malignancy. *Immunity* **28**, 571–580 (2008).
11. Sheppard, S. et al. Characterization of a novel NKG2D and NKp46 double-mutant mouse reveals subtle variations in the NK cell repertoire. *Blood* **121**, 5025–5033 (2013).
12. Gilfillan, S., Ho, E. L., Cella, M., Yokoyama, W. M. & Colonna, M. NKG2D recruits two distinct adapters to trigger NK cell activation and costimulation. *Nat. Immunol.* **3**, 1150–1155 (2002).
13. Lanier, L. L. DAP10- and DAP12-associated receptors in innate immunity. *Immunol. Rev.* **227**, 150–160 (2009).
14. Hamerman, J. A. & Lanier, L. L. Inhibition of immune responses by ITAM-bearing receptors. *Sci. STKE* **2006**, re1 (2006).
15. Arase, H. et al. Negative regulation of expression and function of Fc gamma RIII by CD3 zeta in murine NK cells. *J. Immunol.* **166**, 21–25 (2001).
16. Utsuyama, M. & Hirokawa, K. Radiation-induced-thymic lymphoma occurs in young, but not in old mice. *Exp. Mol. Pathol.* **74**, 319–325 (2003).
17. Overwijk, W. W. & Restifo, N. P. B16 as a mouse model for human melanoma. *Curr. Protoc. Immunol.* **39**, 20.1.1–20.1.29 (2001).
18. Lenartić, M. et al. NKG2D promotes B1a cell development and protection against bacterial infection. *J. Immunol.* **198**, 1531–1542 (2017).
19. Schuster, I. S., Coudert, J. D., Andoniou, C. E. & Degli-Esposti, M. A. "Natural regulators": NK cells as modulators of T cell immunity. *Front. Immunol.* **7**, 235 (2016).
20. Soderquest, K. et al. Cutting edge: CD8+ T cell priming in the absence of NK cells leads to enhanced memory responses. *J. Immunol.* **186**, 3304–3308 (2011).
21. Takeda, K. et al. IFN-γ production by lung NK cells is critical for the natural resistance to pulmonary metastasis of B16 melanoma in mice. *J. Leukoc. Biol.* **90**, 777–785 (2011).
22. Dong, Z. et al. The adaptor SAP controls NK cell activation by regulating the enzymes Vav-1 and SHIP-1 and by enhancing conjugates with target cells. *Immunity* **36**, 974–985 (2012).
23. Glasner, A. et al. Recognition and prevention of tumor metastasis by the NK receptor NKp46/NCR1. *J. Immunol.* **188**, 2509–2515 (2012).
24. Lakshmikanth, T. et al. NCRs and DNAM-1 mediate NK cell recognition and lysis of human and mouse melanoma cell lines in vitro and in vivo. *J. Clin. Invest.* **119**, 1251–1263 (2009).

25. Wensveen, F. M. et al. NK cells link obesity-induced adipose stress to inflammation and insulin resistance. *Nat. Immunol.* **16**, 376–385 (2015).
26. Davis, A. H., Guseva, N. V., Ball, B. L. & Heusel, J. W. Characterization of murine cytomegalovirus m157 from infected cells and identification of critical residues mediating recognition by the NK cell receptor Ly49H. *J. Immunol.* **181**, 265–275 (2008).
27. Coudert, J. D., Scarpellino, L., Gros, F., Vivier, E. & Held, W. Sustained NKG2D engagement induces cross-tolerance of multiple distinct NK cell activation pathways. *Blood* **111**, 3571–3578 (2008).
28. Deng, W. et al. Antitumor immunity. A shed NKG2D ligand that promotes natural killer cell activation and tumor rejection. *Science* **348**, 136–139 (2015).
29. Eckelhart, E. et al. A novel Ncr1-Cre mouse reveals the essential role of STAT5 for NK-cell survival and development. *Blood* **117**, 1565–1573 (2011).
30. Schwenk, F., Baron, U. & Rajewsky, K. A cre-transgenic mouse strain for the ubiquitous deletion of loxP-flanked gene segments including deletion in germ cells. *Nucleic Acids Res.* **23**, 5080–5081 (1995).
31. Challen, G. A., Boles, N., Lin, K. K. & Goodell, M. A. Mouse hematopoietic stem cell identification and analysis. *Cytometry. A.* **75**, 14–24 (2009).
32. Karo, J. M., Schatz, D. G. & Sun, J. C. The RAG recombinase dictates functional heterogeneity and cellular fitness in natural killer cells. *Cell* **159**, 94–107 (2014).
33. Viant, C. et al. SHP-1-mediated inhibitory signals promote responsiveness and anti-tumour functions of natural killer cells. *Nat. Commun.* **5**, 5108 (2014).
34. Wu, N. et al. A hematopoietic cell-driven mechanism involving SLAMF6 receptor, SAP adaptors and SHP-1 phosphatase regulates NK cell education. *Nat. Immunol.* **17**, 387–396 (2016).
35. Chen, L. et al. Discovery of a novel shp2 protein tyrosine phosphatase inhibitor. *Mol. Pharmacol.* **70**, 562–570 (2006).
36. Mandelboim, O. & Porgador, A. NKp46. *Int. J. Biochem. Cell. Biol.* **33**, 1147–1150 (2001).
37. Myers, M. D., Dragone, L. L. & Weiss, A. Src-like adaptor protein down-regulates T cell receptor (TCR)-CD3 expression by targeting TCRzeta for degradation. *J. Cell. Biol.* **170**, 285–294 (2005).
38. Goodfellow, H. S. et al. The catalytic activity of the kinase ZAP-70 mediates basal signaling and negative feedback of the T cell receptor pathway. *Sci. Signal.* **8**, ra49 (2015).
39. Hamerman, J. A., Tchao, N. K., Lowell, C. A. & Lanier, L. L. Enhanced Toll-like receptor responses in the absence of signaling adaptor DAP12. *Nat. Immunol.* **6**, 579–586 (2005).
40. Sjölin, H. et al. DAP12 signaling regulates plasmacytoid dendritic cell homeostasis and down-modulates their function during viral infection. *J. Immunol.* **177**, 2908–2916 (2006).
41. Mulrooney, T. J., Posch, P. E. & Hurley, C. K. DAP12 impacts trafficking and surface stability of killer immunoglobulin-like receptors on natural killer cells. *J. Leukoc. Biol.* **94**, 301–313 (2013).
42. Della Chiesa, M. et al. Evidence that the KIR2DS5 gene codes for a surface receptor triggering natural killer cell function. *Eur. J. Immunol.* **38**, 2284–2289 (2008).
43. Fauriat, C., Ivarsson, M. A., Ljunggren, H. G., Malmberg, K. J. & Michaëlsson, J. Education of human natural killer cells by activating killer cell immunoglobulin-like receptors. *Blood* **115**, 1166–1174 (2010).
44. Carr, W. H. et al. Cutting Edge: KIR3DS1, a gene implicated in resistance to progression to AIDS, encodes a DAP12-associated receptor expressed on NK cells that triggers NK cell activation. *J. Immunol.* **178**, 647–651 (2007).
45. Deng, G. M., Beltran, J., Chen, C., Terhorst, C. & Tsokos, G. C. T cell CD3ζ deficiency enables multiorgan tissue inflammation. *J. Immunol.* **191**, 3563–3567 (2013).
46. Yang, M. et al. K33-linked polyubiquitination of Zap70 by Nrdp1 controls CD8(+) T cell activation. *Nat. Immunol.* **16**, 1253–1262 (2015).
47. Takaki, R., Watson, S. R. & Lanier, L. L. DAP12: an adapter protein with dual functionality. *Immunol. Rev.* **214**, 118–129 (2006).
48. Kiel, M. J. et al. SLAM family receptors distinguish hematopoietic stem and progenitor cells and reveal endothelial niches for stem cells. *Cell* **121**, 1109–1121 (2005).
49. Wang, Y. et al. Long noncoding RNA derived from CD244 signaling epigenetically controls CD8+ T-cell immune responses in tuberculosis infection. *Proc. Natl Acad. Sci. USA* **112**, E3883–E3892 (2015).

Acknowledgements

We thank S. Slavić Stupac, M. Samsa, E. Marinović, A. Miše and K. Mikić for technical assistance. We thank S. Jonjić for discussions and overall support to this work. We thank O. Mandelboim (Hebrew University Hadassah Medical School), M. Colonna (Washington University School of Medicine in St. Louis, St. Louis, MO, USA), M. Busslinger (Research Institute of Molecular Pathology, Vienna, Austria), A. Waisman (Institute of Molecular Biology, Mainz, Germany), D.R. Littman (NYU School of Medicine, New York, NY, USA), J. McGlade (University of Toronto, Toronto, Canada) and K. Rajewsky (MDC Center for Molecular Medicine, Berlin, Germany) for providing mouse lines. This work was supported by an EFIS-IL Short-term Fellowship grant to V.J., European Research Council under the European Union's Seventh Framework Programme (FP/2007–2013)/ERC Grant Agreement no. 311335, Swedish Research Council, Norwegian Research Council, Swedish Foundation for Strategic Research, Wallenberg Foundation, Swedish Cancer Foundation, Swedish Childhood Cancer Foundation, as well as the Stockholm County Council and Karolinska Institutet Center for Innovative Medicine to Y.T.B., Netherlands Organization for Scientific Research (91614029), the European Commission (PCIG14-GA-2013-630827), a University of Rijeka Support grant (865.10.2101) and a Croatian Science Foundation Grant (IP-2016-06-8027) to F.M.W., a European Social Fund grant (HR.3.2.01-0263), University of Rijeka Support grant (803.10.1103) and Croatian Science Foundation grant (IP-2016-06-9306) to B.P. and the grant KK.01.1.1.01.0006, awarded to the Scientific Centre of Excellence for Virus Immunology and Vaccines and co-financed by the European Regional Development Fund.

Author contributions

V.J. carried out most of the experiments and analyzed data. M.Š., I.K., M.L., S.M., B.L. and F.M.W. performed and analyzed experiments. B.P. directed the research. B.P., V.J. and F.M.W. designed experiments and wrote the paper. V.S. and M.P. designed and performed qPCR on NK precursors. T.D.H. and Y.T.B. designed and performed RNA-seq experiments.

Competing interests

The authors declare no competing interests.

Additional information

Supplementary information is available for this paper at https://doi.org/10.1038/s41590-018-0209-9.

Reprints and permissions information is available at www.nature.com/reprints.

Correspondence and requests for materials should be addressed to B.P.

Publisher's note: Springer Nature remains neutral with regard to jurisdictional claims in published maps and institutional affiliations.

Methods

Mice. Mice were strictly age and sex matched within experiments and were held in SPF conditions and handled in accordance with institutional, national and/or EU guidelines. Permission for our experiments was given by Ethical Committee of the Faculty of Medicine, University of Rijeka and Croatian Ministry of Agriculture, Veterinary and Food Safety Directorate ((UP/I-322-01/16-01/16, 525-10/0255-16-7). Mice used in experiments were between 6 and 12 weeks of age. *Klrk1*$^{-/-}$, *Klrk1*$^{fl/fl}$ and *Klrk1*$^{\Delta/\Delta}$ were generated as described previously[9,18]. Wild-type C57BL/6 J (strain 000664), Balb/c (strain 00651) and *Ifng*$^{-/-}$ (strain 002287) mice were from the Jackson Laboratory. *Ncr1*$^{GFP/GFP}$ mice were provided by O. Mandelboim (Hebrew University Hadassah Medical School). *Hcst*$^{-/-}$ and *Tyrobp*$^{-/-}$ mice were provided by M. Colonna (St. Louis, MO). *Rag1*$^{cre/+}$ mice and were provided by M. Busslinger (Vienna, Austria). Rosa26-foxed STOP YFP (*EYFP*$^{Stop\text{-}Flox}$) and iDTR mice were provided by A. Waisman (Mainz, Germany). *Ncr1*^{Cre} and *Cd4*^{Cre} mice were provided by V. Sexl (Vienna, Austria) and D. Littman (New York, NY, USA). *Deleter-cre* mice were kindly provided by K. Rajewsky. *Cd247*$^{-/-}$ mice were from CNRS, Orleans. *Sla*$^{-/-}$ mice were provided by J. McGlade (Toronto, Canada). *Klrk1*$^{-/-}$ or *Tyrobp*$^{-/-}$ and wild-type littermates were generated by interbreeding heterozygous mice.

Cells. B16 cell line was purchased from the American Type and Culture Collection (ATCC). Cells were cultured in complete DMEM, supplemented with 10 mM HEPES (pH 7.2), 2 mM L-glutamine, 105 U/L Penicillin, 0.1 g/L Streptomycin, and 10% FCS. Cells were maintained in an incubator at 37 °C and 5% CO_2.

Tumor models. *Radiation induced thymic lymphomas.* Young mice (4–6 weeks old) received low doses of γ radiation (1,6 Gy) once a week for 4 weeks as previously described[16]. In these experiments we used ten mice per group, and experiments were repeated two times.

B16 melanoma. Mice received 10^5 B16 clone F10 (B16) cells i.v or s.c and survival (reaching of human end points) or tumor growth, respectively, was followed. Digital caliper was used to measure tumor size. X-ray pictures of tumors in isolated skin were done using an in vivo imager (MS FX Pro, Carestream) on day 10 after s.c. tumor inoculation. To deplete lymphocyte populations, mice received 250 μg antibodies i.p. 1 d before tumor inoculation and repeated every fifth day. Antibodies used were αCD4 (YTS 191.1.2), αCD8 (YTS 169.4.2) and αNK1.1 (PK136). In these experiments we used ten mice per group and experiments were repeated at least two times.

In vitro analysis of NK cells. For NK killer assay, B16 cells were labeled with CFSE and co-cultured with C57BL/6 J or *Klrk1*$^{-/-}$ splenocytes, respectively, at an effector to-target ratio adjusted to the number of NK cells. After 4 h or 14 h co-culture in a 5% CO_2 atmosphere at 37 °C, specific lysis was determined in triplicate by flow cytometric analysis as measured by To-pro-3 (To-pro-3 iodide, Life technologies) incorporation. Spontaneous death of cells was determined in wells containing targets only[9]. In co-cultivation assays for cytokine production analysis, splenocytes from WT or *Klrk1*$^{-/-}$ mice were co-cultured with B16 cells in a 1:1 ratio overnight at 5% CO_2 at 37 °C with IL-2 (100 U/mL, R&D Systems), IL-12 (50 pg, R&D Systems) and addition of Brefeldin A (eBioscience) for the last 4 h. IFN-γ production by NK cells was analyzed by flow cytometry. Formation of conjugates was done as previously described[22]. Briefly, B16 cells were CFSE labeled and co-cultured with NK1.1-labeled splenocytes. At indicated time points, the fraction of CFSE$^+$NK1.1$^+$ double positive cells was determined by flow cytometry. For in vitro NK cell stimulations and analysis of cytokine production 5×10^5 splenocytes were stimulated for 4 h at 5% CO_2 atmosphere and 37 °C in addition to IL-2 (100 U, Preprotech) and Brefeldin A (eBioscience). For stimulation through specific activating receptor 2–5 μg/mL of antibody in PBS was pre-coated on an ELISA plate (αLy49H (3D10), αLy49D (4e4), αNK1.1 (PK136), αNCR1 (29A1.4) and IgG2aκ (eBM2a)). Cytokines were added in suspension: IL-12 (10 ng/mL, R&D Systems) and IL-18 (20 ng/mL, R&D Systems). For SHP-1/2 inhibition we cultured cells in the presence of 50 μM SHP-1/2 PTPase inhibitor (NSC-87877, Merck Millipore) dissolved in DMSO, or DMSO only as control. In experiments of in vitro NK cell analysis we used five mice per group and experiments were repeated two to three times.

Phosphorylation kinetics. Splenocytes were starved from stimuli in RPMI 1640 for 30 min at 37 °C in a humidified incubator with 5% CO_2. Next, cells (5×10^5) were stimulated with 2 μg/mL αNCR1 (29A1.4) for the indicated times. Cells were fixed with 2% paraformaldehyde, permeabilized in 90% methanol, and stained with p-Syk (Y348) (moch1ct, eBioscience) or p-PLC-γ1(Y783) (D6M9S, Cell Signaling). In these experiments 4–5 mice per group were used and experiment were repeated two to three times.

Purification of NK cells and RNA isolation for qPCR. NK cells were enriched from splenocytes using biotinylated DX5 antibodies, streptavidin-coated beads and magnetic cell sorting (Milteny). Next, NK cells (CD3$^-$NK1.1$^+$) were sorted to high (>99% purity) on a FACS Aria II (BD Biosciences). RNA was isolated via the Trizol method, and cDNA was generated with a reverse transcriptase core kit (Eurogentec). The expression of mRNA was examined by quantitative PCR analysis with a 7500 Fast Real Time PCR machine. Taqman assays were used to quantify the expression of *Ifng* (IFN-γ, Mm00485148_m1). The relative mRNA expression was normalized by quantification of Rn18S (18S, Mm03928990_g1) RNA in each sample.

RNA-seq. Sorted cells were stored frozen in RLT buffer (Qiagen). Lysates were thawed and RNA extracted using column-based purification with the inclusion of a DNase I treatment (TurboDNase, Ambion, Thermo Fischer Scientific). Purified RNA was converted to cDNA using Superscript II kit with the addition of 20 ng/ml anchored Oligo d (T) (Thermo Fischer Scientific) and 1 M Betaine, 12 m M $MgCl_2$ (Sigma-Aldrich) to aid conversion. Second-strand cDNA synthesis proceeded directly using the NEB second strand cDNA synthesis kit (New England BioLabs Ltd). The completed cDNA reaction was transferred to a Covaris AFA tube and sonicated using 140 W peak power at 200 cycles for 3 min to generate average length fragments of 300 bp (Covaris S220, Covaris Inc.). DNA was extracted (Micro DNA columns, Qiagen) and used as template in Illuminia compatible sequencing library preparation kit (DNA-seq Thruplex, Rubicon Genomics). Multiplexed libraries were purified twice using AMPure beads (Becton Coulter Inc.) and quantified using Qubit (Thermo Fischer Scientific) and Kapa Library Quantification (Kapa Biosystems). Sequencing was performed on a Hi-Seq 3000 (Illuminia, USA). Sequencing reads were FASTQ quality assessed, trimmed using trim galore and mapped to the mm10 mouse genome assembly using STAR-SEQ. Differential expression analysis was accomplished using limma and edgeR R programmes. For qualified cluster analysis, genes differentially expressed between C57BL/6 J and Klrk1 NK cells were analyzed using the String (http://www.String-db.org) database to identify associations with Zap70 and CD247. Network edges with a confidence interval of 0.4 are included, whereas unconnected nodes were excluded. Clustering was visualized using Cytoscape 3.5.0 software.

Purification of NK cell precursors and RNA isolation for qPCR. NK precursors (stage 1 and stage 2) were sorted according to their expression profiles described in supplementary Fig. 4a. Total RNA was extracted using RNeasy Micro Kit (Qiagen). The quality of the RNA obtained was evaluated using the Laboratory-Chip technique (Agilent Bioanalyzer) and subsequently preamplified according to the Ambion WTA expression protocol (Thermo Fischer). RNA was reverse transcribed into cDNA using the iScript protocol (Bio-Rad). QT-PCR was performed using the SsoAdvanced Universal SYBR Green Supermix (Bio-Rad) and the MyCycler Thermal cycler system (Bio-Rad).The following primers were used: mNKG2D-S FW: AGTTGAGTTGAAGGCTTTGACTC, mNKG2D-S REV: ACTTTGCTGGCTTGAGGTC, DAP12 FW: GACTGTGGGAGGATTAAGTCC, DAP12 REV: AACACCAAGTCACCCAGAAC.

Flow cytometry. Cells were pretreated with Fc block (clone 2.4G2, produced in-house). To-pro3 (life Technologies) or Fixable Viability Dye (eBioscience) was used to exclude dead cells. Cells were stained and analyzed in PBS containing 1% BSA and NaN3 with antibodies listed below. For intracellular staining, permeabilization and fixation of cells was done with the Fix/Perm kit (BD Biosciences).The cells were measured on a FACSVerse or FACSAria flow cytometer (BD Biosciences), and data were analyzed using FlowJo v10 software (Tree Star, Ashland, OR). To analyze ligands expression tumor cells were stained with fusion proteins (NKG2D-Fc or NCR1-Fc) or irrelevant fusion protein and secondary FITC labeled anti-human antibody. For flow cytometry, we used monoclonal antibodies to mouse CD3e (145-2C11), NK1.1 (PK136), CD49b (DX5), IFN-γ (XMG1.2), TNFα (MP6-XT22), IL-6 (MP5-32C11), GM-CSF (MP1-22E9), NKG2D (CD314) (CX5), CD247 (CD3ζ) (6B10.2), ZAP-70 (1E7.2), CD122 (TM-b1), CD11b (M1/70) and c-kit (CD117) (ACK2) from eBioscience. FcεR1γ (1D6) from MBL, CD247 (CD3ζ) (H146-968) from Abcam. Ly49H (3D10) and Ly49D (4e4) were kind gift from W. Yokoyama (Washington University in St. Louis, USA). For hematopoietic stem cell staining, bone marrow cells were stained with Abs against CD34 (RAM34), Flt3L (A2F10.1), CD127 (A7R34), CD16/32 (93), Sca1 (D7), and CD117 (2B8). Populations were defined according to previous publication[31] as following CLP (CD117^{dim}Sca1^{dim}Flt3L$^+$CD127$^+$),PreProNK (CD117^{dim}Sca1^{2+}Flt3L$^-$CD127$^+$), MPP (CD117$^+$Sca1$^+$CD34$^+$Flt3L$^+$), ST-HSC (CD117$^+$Sca1$^+$CD34$^+$Flt3L$^-$), LT-HSC (CD117$^+$Sca1$^+$CD34$^-$Flt3L$^-$), CMP (CD117$^+$Sca1$^-$CD34$^+$CD16^{int}), GMP (CD117$^+$Sca1$^-$CD34$^+$CD16$^+$), MEP (CD117$^+$Sca1$^-$CD34$^-$CD16$^-$). Biotinylated Abs against CD4 (GK1.5), CD8 (53-6.7), B220 (RA3-6B2), Gr-1 (RB6-8C5), CD11b (M1/70), TER119 (Ter-119), NK.1.1 (PK136) were used to exclude Lin$^+$ cells. In experiment where we analyzed 6 stages of NK cell development NK1.1 (PK136) was excluded from staining for Lin$^+$ cells. Abs were purchased from eBioscience or BD Biosciences. Fusion proteins (NCR1-Fc, NKG2D-Fc and hPVR-Fc) were produced by our in-house facility.

MCMV infection. The tissue culture grown mCMV MW97.01 and *Δm157* MCMV was produced in mouse embryonic fibroblasts according to standard protocol. The mice were either treated with αNK1.1 (PK136, 250 μg/mouse) or PBS 24 h before i.v. injection of 5×10^5 PFU of *Δm157* MCMV. Four days after infection mice were sacrificed, and viral titers were determined in spleens by standard virus plaque assay. In these experiments 4–5 mice per group were used and experiment were repeated two to three times.

In vivo NKG2D blocking. *Rag1*^{Cre}*EYFP*$^{Stop\text{-}Flox}$iDTR mice were injected i.p. on two consecutive days with 0.8 mg diphtheria toxin. From the second day onwards, mice received once every 3 d 200 µg anti-NKG2D (BioXcell, clone HMG2D) or istotype control antibodies. After 15 d, spleens and bone marrow were analyzed.

ImmunoBlot. NK cells were enriched from splenocytes using MACS and then sorted o high (>99% purity) on a FACS Aria II (BD Biosciences). Cell extracts were generated using laemmli sample buffer (Syk, FcR1γ and Zap 70) or RIPA buffer (CD3ζ), in the presence of protease inhibitors (complete Ultra, Roche). Equal amounts of total lysate were analyzed by 12% SDS–PAGE. Proteins were transferred to Immobilon-P and incubated with blocking buffer (Tris buffered saline/Tween-20) containing 2% low-fat milk for 1 h before incubating with an antibody against Syk (Cell Signaling), FcR1γ (Merck Millipore), Zap-70 (Cell Signaling) and CD3ζ (Sigma), Akt (Cell signaling) or β-actin (Santa Cruz). Bands were visualized with ECL Prime Immuno Blotting Detection Reagent (GE Healthcare) using ImageQuant LAS 4000mini (GE Healthcare, Life Science).

Quantitation and statistical analysis. To analyze statistical significance, we used Student's *t*-test, Mann–Whitney, Kruskal–Wallis and ANOVA, with Bonferroni's post-test correction for multiple comparisons. To assess survival rates, the Kaplan–Meier model was used followed by log-rank (Mantel–Cox) test for pairwise group comparisons. Statistical significance is defined as: * $P<0.05$; ** $P<0.01$; *** $P<0.001$.

Reporting Summary. Further information on research design is available in the Nature Research Reporting Summary linked to this article.

Data availability

The data that support the findings of this study are available from the corresponding author upon request. The NCBI SRA accession codes are: SRX4548789, SRX4548788, SRX4548787, SRX4548786, SRX4548785, SRX4548784, SRX4548783, SRX4548782, SRX4548781.

nature research

Corresponding author(s): Bojan Polić

Reporting Summary

Nature Research wishes to improve the reproducibility of the work that we publish. This form provides structure for consistency and transparency in reporting. For further information on Nature Research policies, see Authors & Referees and the Editorial Policy Checklist.

Statistical parameters

When statistical analyses are reported, confirm that the following items are present in the relevant location (e.g. figure legend, table legend, main text, or Methods section).

n/a	Confirmed	
☐	☒	The exact sample size (*n*) for each experimental group/condition, given as a discrete number and unit of measurement
☐	☒	An indication of whether measurements were taken from distinct samples or whether the same sample was measured repeatedly
☐	☒	The statistical test(s) used AND whether they are one- or two-sided *Only common tests should be described solely by name; describe more complex techniques in the Methods section.*
☒	☐	A description of all covariates tested
☐	☒	A description of any assumptions or corrections, such as tests of normality and adjustment for multiple comparisons
☐	☒	A full description of the statistics including central tendency (e.g. means) or other basic estimates (e.g. regression coefficient) AND variation (e.g. standard deviation) or associated estimates of uncertainty (e.g. confidence intervals)
☐	☒	For null hypothesis testing, the test statistic (e.g. *F*, *t*, *r*) with confidence intervals, effect sizes, degrees of freedom and *P* value noted *Give P values as exact values whenever suitable.*
☒	☐	For Bayesian analysis, information on the choice of priors and Markov chain Monte Carlo settings
☒	☐	For hierarchical and complex designs, identification of the appropriate level for tests and full reporting of outcomes
☒	☐	Estimates of effect sizes (e.g. Cohen's *d*, Pearson's *r*), indicating how they were calculated
☐	☒	Clearly defined error bars *State explicitly what error bars represent (e.g. SD, SE, CI)*

Our web collection on statistics for biologists may be useful.

Software and code

Policy information about availability of computer code

Data collection	N.A.
Data analysis	Flow Cytometry data analysis was performed using FlowJo software (Tree Star, version 10) For qualified cluster analysis we used String (www.String-db.org) Clustering of differentially expressed genes was visualized using Cytoscape 3.5.0 software Statistical analysis between groups was performed with GraphPad Prism 5 and 7 Differential expression analysis was done using EdgeR 3.14.2 and Limma 3.28.1 In data analysis MS Excel was also used

For manuscripts utilizing custom algorithms or software that are central to the research but not yet described in published literature, software must be made available to editors/reviewers upon request. We strongly encourage code deposition in a community repository (e.g. GitHub). See the Nature Research guidelines for submitting code & software for further information.

Data

Policy information about availability of data

All manuscripts must include a data availability statement. This statement should provide the following information, where applicable:

- Accession codes, unique identifiers, or web links for publicly available datasets
- A list of figures that have associated raw data
- A description of any restrictions on data availability

The data that support the findings of this study are available from the corresponding author upon request. The accession codes are: SRX4548789, SRX4548788, SRX4548787, SRX4548786, SRX4548785, SRX4548784, SRX4548783, SRX4548782, SRX4548781

Field-specific reporting

Please select the best fit for your research. If you are not sure, read the appropriate sections before making your selection.

☒ Life sciences ☐ Behavioural & social sciences ☐ Ecological, evolutionary & environmental sciences

For a reference copy of the document with all sections, see nature.com/authors/policies/ReportingSummary-flat.pdf

Life sciences study design

All studies must disclose on these points even when the disclosure is negative.

Sample size	Sample size was determined by power analysis based on pilot experiments and previous findings (Zafirova et. al.,Immunity 2009.)
Data exclusions	No data was excluded
Replication	All data was successfully replicated at least two times. How many times each experiment was performed and which statistical analysis was used is indicated in the figure legends.
Randomization	Mice were age and sex matched. Mice were allocated to groups by an independent animal caretaker.
Blinding	In our experiments we used mostly genetically modified mice which were genotyped before start of each experiment to determine appropriate number of animals per group to ensure statistical power of results for each experiment. However, individual mice and from them derived samples were numbered regardless of genotype, which finally allowed blind analysis of samples though. The samples were matched with their genotype only after the analysis.

Reporting for specific materials, systems and methods

Materials & experimental systems

n/a	Involved in the study
☒	☐ Unique biological materials
☐	☒ Antibodies
☐	☒ Eukaryotic cell lines
☒	☐ Palaeontology
☐	☒ Animals and other organisms
☒	☐ Human research participants

Methods

n/a	Involved in the study
☒	☐ ChIP-seq
☐	☒ Flow cytometry
☒	☐ MRI-based neuroimaging

Antibodies

Antibodies used

Flow Cytometry:
Name / Clone name / Catalog no. / (most used) Lot no. / dilution factor / manufacturer
CD3e/145-2C11/ 45003182/4304569/1:300/eBioscience
NK1.1/PK136/45594182/l4331619/1:400/eBioscience
CD49b/DX5/13597183/E03102-1631/1:100/eBioscience
FNγ/XMG1.2/17731182/4332526/1:200/eBioscience
TNFα /MP6-XT22/11732181/1927449/1:100/eBioscience
IL-6/8C9 /21670064/LO144/1:100/Immuno tools
GM-CSF/MP1-22E9/12-7331-41/E031118/1:100/eBioscience

NKG2D (CD314)/CX5/25-5882-82/4275095/1:50/eBioscience
CD247 (CD3ζ)/6B10.2/12-2479-80/4291757/1:50/eBioscience
ZAP-70/1E7.2/11-6695-82/4308883/1:400/eBioscience
CD122 /TM-b1/17-1222-80/E004801633/1:100/eBioscience
CD11b/M1/70/ 25011281/4289817/1:400/eBioscience
c-kit (CD117)/ACK2/11-1171-82/E004741631/1:100/eBioscience
FcεR1γ /1D6/M191-3/ 1:100/MBL
CD247 (CD3ζ)/H146-968/ ab91493/6R3198401-1/1:100/ Abcam.
Ly49H (3D10) and Ly49D (4e4) were kind gift from W. Yokoyama (Washington University in St. Louis, USA)/1:100
CD34 /RAM34/14-0341-81/E02497-1631/1:100/eBioscience
Flt3L /A2F10.1/17-1351-80/E02731-1633/1:100/eBioscience
CD127 /A7R34/14-1271-82/E014711633/1:100/eBioscience
CD16/32 /93/14-0161-81/E06356-1631/1:100/eBioscience
Sca1/D7/17598181/E073531635/1:100/eBioscience
pSyk(Y348)/moch1ct/12901442/4325047
pPLCγ(Y786M9S/14008/1:400/Cell Signaling
Sla/rabbit polyclonal/PA5-22356/TA2506553/1:50/Invitrogen
Fusion proteins (NCR1-Fc, NKG2D-Fc and hPVR-Fc) were produced by our in-house facility and used 10µg/sample

Western blot:
Name / Clone name / Catalog no. / (most used) Lot no. / dilution factor / manufacturer
Syk/D3Z1E/3198/2/1:1000/Cell signaling
FcR1γ/rabbit polyclonal/06-727/2882662/1:500/ Merckmillipore
Zap70/99F2/2705/10/1:500/Cell signaling
CD3ζ /rabbit polyclonal/SAB4503580/210468/1:500/Sigma
Akt /11E7/4685/6/1:80000/Cell signaling
β-actin/C4/MAB/2665057/1:80000/Santa Cruz

Validation

Validation of purchased antibodies was done by the suppliers. Data on the validation of in-house generated reagents (fusion proteins), has been provided in the supplementary figures.

Eukaryotic cell lines

Policy information about cell lines

Cell line source(s)

The B16-F10 cell line was purchased from ATCC (CRL-6475)

Authentication

Authentication was provided by ATCC

Mycoplasma contamination

The cell line was confirmed to be negative for mycoplasma contamination by PCR.

Commonly misidentified lines
(See ICLAC register)

No commonly misidentified cell lines were used.

Animals and other organisms

Policy information about studies involving animals; ARRIVE guidelines recommended for reporting animal research

Laboratory animals

Mice used in experiments were 6-12 weeks old. Both male and female mice were used but they were strictly age- and sex-matched within experiments.
Klrk1-/- Zafirova et al., 2009.
Klrk1flox/flox Lenartić et al., 2017.
Klrk1Δ/Δ Zafirova et al., 2011.
NCR1gfp/gfp Gazit et al., 2006.
IFNγ-/- Jackson Laboratories(2287)
C57BL/6 Jackson Laboratories (B6; strain 664)
Hcst-/- Laboratory of M. Colonna
Tyrobp-/- Laboratory of M. Colonna
Rag1cre/+ Laboratory of M. Busslinger
Rosa26-foxed STOP YFP Laboratory of Ari Waisman
NCR1cre Laboratory of V. Sexl
CD4cre Laboratory of D. Littman
CD3ζ-/- CNRS, Orleans (B6-Cd3z tm1Mal)
Deleter-cre (B6.C-Tg(CMV-cre)1Cgn/J) Jackson Laboratories (6054)
Balb/c Jackson Laboratories (strain 00651)
Sla-/- Laboratory of Jane McGlade4)

Wild animals

Study did not involve wild animals

Field-collected samples

Study did not involve samples collected from the field

Flow Cytometry

Plots

Confirm that:

☒ The axis labels state the marker and fluorochrome used (e.g. CD4-FITC).

☒ The axis scales are clearly visible. Include numbers along axes only for bottom left plot of group (a 'group' is an analysis of identical markers).

☒ All plots are contour plots with outliers or pseudocolor plots.

☒ A numerical value for number of cells or percentage (with statistics) is provided.

Methodology

Sample preparation	Samples were prepared as described in the methods section. Briefly, animals were sacrificed according to European guidelines and spleens and bone marrow were removed. Single cell suspensions were generated by mashing organs through a 70uM sieve (spleen) or by smashing bones with a mortar, after which suspensions were run through a sieve. Erythrocytes were lysed using a hypotonic solution. Before staining with specific antibodies, cells were pretreated with Fc block (clone 2.4G2, produced in-house). To-pro3 (life Technologies) or Fixable Viability Dye (eBioscience) was used to exclude dead cells.
Instrument	BD FACS ARIA and BD FACS VERSE
Software	FlowJo software (Tree Star, version 10)
Cell population abundance	After sorting we purity was determined to be 97-99%.
Gating strategy	pecific gating strategies are specified in the figure legends and/or methods section. Briefly, doublets were excluded using FSC-H vs. FSC-A gating, followed by SSC-H vs. SSC-A gating. Dead cells were excluded by viability dye. Based on FSC/SSC properties gating for lymphocytes was performed. Next, markers for specific cell populations were used to define populations. In most experiments, murine NK cells were investigated, which were defined as CD3-NK1.1+ or CD3-NKp46+, depending on the experiment and/or genotype of the mice under investigation. For cytokine production or for specific marker expression, positive gates were set based on isotype control, FMO, or on cells genetically deficient for the specified marker (e.g. NKG2D, NCR1, CD3zeta). For analysis of haematopoietic precursors in the bone marrow, a lineage channel was used, as well as specific markers to define precursor populations.

☒ Tick this box to confirm that a figure exemplifying the gating strategy is provided in the Supplementary Information.